DOI: 10.1021/ic100063c

Inorganic Chemistry
Article

Cyclometalated Ru Complexes of Type $[Ru^{II}(N^{\wedge}N)_2(C^{\wedge}N)]^z$: Physicochemical Response to Substituents Installed on the Anionic Ligand

Paolo G. Bomben, Bryan D. Koivisto, and Curtis P. Berlinguette*

Department of Chemistry and The Institute for Sustainable Energy, Environment and Economy, University of Calgary, 2500 University Drive N.W., Calgary, Canada T2N 1N4

Received January 11, 2010

The electrochemical and photophysical properties of a series of Ru(II) complexes related to $[Ru(dcbpyH_2)_2(ppy)]^{1+}$ (**1**; dcbpy-H_2 = 4,4′-dicarboxy-2,2′-bipyridine; ppy = 2-phenylpyridine) were examined to elucidate the effect of modifying the anionic fragment of the $C^{\wedge}N$ ligand with conjugated substituents (R). Included in this study is a family of compounds (**2**−**5**) consisting of one or two $-NO_2$ groups installed *meta*, *ortho*, and *para* to the organometallic bond. A suite of compounds with electron-donating and withdrawing groups (e.g., R = −F (**6**), −phenyl (**7**), −4-pyridine (**8**), −thiophene-2-carbaldehyde (**9**)) were also evaluated. Deprotonated forms of select compounds were isolated as tetrabutylammonium salts to benefit solution studies. All complexes were structurally characterized by a combination of mass spectrometry, ^1H and ^{13}C NMR spectroscopy, and/or elemental analysis. The electronic absorption spectra for all of the compounds reveal three broad bands over the 350−700 nm range. The maximum wavelength of the lowest energy absorbance bands for complexes modified with electron-withdrawing groups are hypsochromically shifted up to 45 nm relative to **1**; the weakly emitting compounds (i.e., **1**, **3**, **6**−**9**) display a hypsochromic shift of up to 63 nm compared to **1**. Emission was not observed in cases where the $-NO_2$ group was positioned *meta* to the Ru−C bond. The sensitivity of the oxidation potentials to the nature, number, and position of the electron-withdrawing/-donating substituents for the entire set of compounds reflect a highest occupied molecular orbital (HOMO) character extended over the metal, the anionic portion of the $C^{\wedge}N$ ligand, and, in the case of **7**−**9**, the conjugated R group. The reduction potentials indicate that the lowest unoccupied molecular orbital (LUMO) is localized to the $C^{\wedge}N$ ligand where R = $-NO_2$, and on the dcbpyH_2 ligands for all other compounds. This assessment was corroborated by time-dependent density functional theory (TD-DFT) studies.

Introduction

The design and study of polypyridyl Ru(II) complexes is fueled by the vast utility of this class of compounds in a myriad of applications (e.g., solar cells,[1] artificial photosynthetic schemes,[2,3] sensors[4,5]). The versatility of these complexes is a consequence of their favorable redox properties, chemical stability, luminescence behavior, and excited-state reactivity.[6−12] The development of cyclometalated Ru(II) congeners, however, has received far less attention in the context of photochemical studies.[13−23] This observation is

*To whom correspondence should be addressed. E-mail: cberling@ucalgary.ca.

(1) Grätzel, M. *Inorg. Chem.* **2005**, *44*, 6841–6851.
(2) Concepcion, J. J.; Jurss, J. W.; Brennaman, M. K.; Hoertz, P. G.; Patrocinio, A. O. T.; Murakami Iha, N. Y.; Templeton, J. L.; Meyer, T. J. *Acc. Chem. Res.* **2009**, *42*, 1954–1965.
(3) Wasylenko, D. J.; Ganesamoorthy, C.; Koivisto, B. D.; Henderson, M. A.; Berlinguette, C. P. *Inorg. Chem.* **2010**, *49*, 2202–2209.
(4) Beer, P. D.; Cadman, J. *Coord. Chem. Rev.* **2000**, *205*, 131–155.
(5) Vos, J. G.; Kelly, J. M. *Dalton Trans.* **2006**, 4869–4883.
(6) Juris, A.; Balzani, V.; Barigelletti, F.; Campagna, S.; Belser, P.; Von Zelewsky, A. *Coord. Chem. Rev.* **1988**, *84*, 85–277.
(7) Campagna, S.; Puntoriero, F.; Nastasi, F.; Bergamini, G.; Balzani, V. *Top. Curr. Chem.* **2007**, *280*, 117–214.
(8) Angell, S. E.; Zhang, Y.; Rogers, C. W.; Wolf, M. O.; Jones, W. E. *Inorg. Chem.* **2005**, *44*, 7377–7384.
(9) Medlycott, E. A.; Hanan, G. S. *Chem. Soc. Rev.* **2005**, *34*, 133–142.
(10) Kuciauskas, D.; Monat, J. E.; Villahermosa, R.; Gray, H. B.; Lewis, N. S.; McCusker, J. K. *J. Phys. Chem. B* **2002**, *106*, 9347–9358.
(11) Del Guerzo, A.; Leroy, S.; Fages, F.; Schmehl, R. H. *Inorg. Chem.* **2002**, *41*, 359–366.
(12) Wang, X.-Y.; Del Guerzo, A.; Tunuguntla, H.; Schmehl, R. H. *Res. Chem. Intermed.* **2007**, *33*, 63–77.
(13) Constable, E. C.; Hannon, M. J. *Inorg. Chim. Acta* **1993**, *211*, 101–110.
(14) Constable, E. C.; Thompson, A. M. W. C.; Tocher, D. A.; Daniels, M. A. M. *New J. Chem.* **1992**, *16*, 855–867.
(15) Constable, E. C.; Housecroft, C. E. *Polyhedron* **1990**, *9*, 1939–1947.
(16) Constable, E. C.; Leese, T. A. *J. Organomet. Chem.* **1987**, *335*, 293–299.
(17) Constable, E. C.; Holmes, J. M. *J. Organomet. Chem.* **1986**, *301*, 203–208.
(18) Reveco, P.; Cherry, W. R.; Medley, J.; Garber, A.; Gale, R. J.; Selbin, J. *Inorg. Chem.* **1986**, *25*, 1842–1845.
(19) Patoux, C.; Launay, J.-P.; Beley, M.; Chodorowski-Kimmes, S.; Collin, J.-P.; James, S.; Sauvage, J.-P. *J. Am. Chem. Soc.* **1998**, *120*, 3717–3725.
(20) Ott, S.; Borgström, M.; Hammarström, L.; Johansson, O. *Dalton Trans.* **2006**, 1434–1443.
(21) Djukic, J. P.; Sortais, J. B.; Barloy, L.; Pfeffer, M. *Eur. J. Inorg. Chem.* **2009**, 817–853.
(22) Gandolfi, C.; Heckenroth, M.; Neels, A.; Laurenczy, G.; Albrecht, M. *Organometallics* **2009**, *28*, 5112–5121.
(23) Sasaki, I.; Vendier, L.; Sournia-Saquet, A.; Lacroix, P. G. *Eur. J. Inorg. Chem.* **2006**, 3294–3302.

Published on Web 05/17/2010

presumably because the requisite C−H activation step renders the synthesis of cyclometalated systems more onerous and/or because luminescence is usually compromised when the dative Ru−N bond is replaced by a Ru−C bond.[21,24] Notwithstanding, the accessibility of these compounds has increased because of the development of new synthetic methodologies, and it has been shown that the strongly σ-donating cyclometalating ligand promotes a unique set of photophysical properties.[15,17,25−28] A notable recent advance is the recognition by van Koten et al., that tridentate cyclometalated Ru(II) chromophores can generate reasonable power conversion efficiencies in the dye-sensitized solar cell (DSSC[1]).[29] This finding was followed up by a report by Grätzel et al., documenting a cell power conversion efficiency (η) of 10.1% using the $C^\wedge N$ complex, $[Ru(dcbpyH_2)_2(\mathbf{L6})]^+$ ($dcbpyH_2$ = 4,4′-dicarboxy-2,2′-bipyridine; **HL6** = 2-(2,4-difluorophenyl)pyridine).[30] This complex, which represents the first "champion" (i.e., $\eta > 10\%$) dye devoid of NCS^- groups, provides the imperative to study these compounds in further detail.

The highest occupied molecular orbital (HOMO) of cyclometalated complexes of type $[Ru(N^\wedge N^\wedge N)(N^\wedge N^\wedge C)]^+$ and $[Ru(N^\wedge N)_2(C^\wedge N)]^+$ is typically extended over the metal and, to a lesser extent, the anionic portion of the cyclometalating ligand.[15,31−36] The lowest-unoccupied molecular orbital (LUMO) typically resides on the neutral polypyridyl ligands along with low-lying excited states delocalized over the pyridyl portion(s) of the cyclometalating ligand. This scenario leads to a series of broad absorption bands in the visible region of the spectrum that arise primarily from mixed-metal/ligand-to-ligand charge-transfer transitions. These electronic transitions have important implications in light-harvesting applications because it offers the opportunity to manipulate the redox behavior and optical properties by selectively tuning the LUMO and HOMO energy levels (Figure 1).[35]

Taking these observations into account, we have set out to examine how the photophysical and electrochemical properties of $[Ru(dcbpyH_2)_2(\mathbf{L1})]^+$ (**1**; **HL1** = 2-phenylpyridine) are affected when various substituents (e.g., $-NO_2$, −F, −phenyl, −4-pyridine, −thiophene-2-carbaldehyde) are installed on the phenyl ring of the cyclometalating ligand

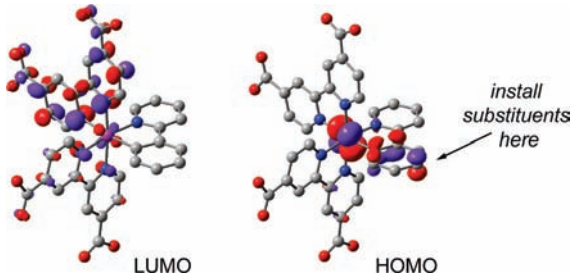

Figure 1. Frontier molecular orbitals of **1** illustrating our motivation to install substituents on the phenyl ring of the $C^\wedge N$ ligand to achieve optimal interaction with the HOMO. (Color scheme: Ru = purple; N = blue; O = red; C = gray; H atoms not shown.).

(Figure 2 and Chart 1). This study is designed to gain a specific understanding of how *conjugated* substituents interact with the HOMO of **1**. Our curiosity is driven by the notion that expanding the orbital character of the HOMO over the conjugated substituents should produce a superior absorption envelope for light-harvesting applications. The isolation and study of the series **2**−**5** confirm that the presence of the $-NO_2$ groups can, indeed, increase the broadness and intensity of the absorption bands relative to **1** and **6**. Because this group is not ideal for applications that require excited-state reactivity, we replaced the quenching $-NO_2$ groups with aromatic substituents to form **7**−**9**. It is found that the thiophene-based substituent of **9** is a particularly effective means of improving the optical properties relative to **1**. The polypyridyl ligand of choice in this study is $dcbpyH_2$ because the utility of these metal complexes as sensitizers often requires a mode for binding to a semiconducting material (e.g., TiO_2 in the DSSC). The electrochemical and photophysical properties of these complexes are detailed herein, as well as the identification of an efficient preparative route for isolating cyclometalated Ru(II) complexes.

Experimental Section

Preparation of Compounds. All manipulations were performed using solvents passed through an MBraun solvent purification system prior to use; chloroform ($CHCl_3$) and tetrahydrofuran (THF) solvents were of analytical grade (without stabilizer). All reagents were purchased from Aldrich, except for $RuCl_3$ (Pressure Chemical Company), bpy and $dcbpyH_2$ (Alfa Aesar). Ligands **HL1** (2-phenylpyridine) and **HL6** (2-(2,4-difluorophenyl)pyridine) and phenylboronic acid were used as supplied from Aldrich. Purification by column chromatography was carried out using silica (Silicycle: Ultrapure Flash Silica), basic alumina (Fluka), or Sephadex LH-20 (Pharmacia). Analytical thin-layer chromatography (TLC) was performed on aluminum-backed sheets precoated with silica 60 F254 adsorbent (0.25 mm thick; Merck, Germany) or with plastic-backed sheets precoated with basic alumina 200 F254 adsorbent (0.25 mm thick, Selecto Scientific: Georgia, U.S.A.) and visualized under UV light. ^{1}H NMR chemical shifts (δ) are reported in parts per million (ppm) from low to high field and referenced to residual non-deuterated solvent. Standard abbreviations indicating multiplicity are used as follows: s = singlet; d = doublet; t = triplet; m = multiplet. A labeling scheme for the ^{1}H NMR assignments of selected ligands are provided in Supporting Information.

2-(3-(4,4,5,5-Tetramethyl-1,3,2-dioxaborolan-2-yl)phenyl)-pyridine:[37] A THF solution containing 2.51 g (10.7 mmol) of

(24) Chi, Y.; Chou, P.-T. *Chem. Soc. Rev.* **2007**, *36*, 1421–1431.
(25) Collin, J. P.; Beley, M.; Sauvage, J. P.; Barigelletti, F. *Inorg. Chim. Acta* **1991**, *186*, 91–93.
(26) Ryabov, A. D.; Sukharev, V. S.; Alexandrova, L.; Le Lagadec, R.; Pfeffer, M. *Inorg. Chem.* **2001**, *40*, 6529–6532.
(27) Fernandez, S.; Pfeffer, M.; Ritleng, V.; Sirlin, C. *Organometallics* **1999**, *18*, 2390–2394.
(28) Wade, C. R.; Gabbai, F. P. *Inorg. Chem.* **2010**, *49*, 714–720.
(29) Wadman, S. H.; Kroon, J. M.; Bakker, K.; Lutz, M.; Spek, A. L.; van Klink, G. P. M.; van Koten, G. *Chem. Commun.* **2007**, 1907–1909.
(30) Bessho, T.; Yoneda, E.; Yum, J.-H.; Guglielmi, M.; Tavernelli, I.; Imai, H.; Rothlisberger, U.; Nazeeruddin, M. K.; Grätzel, M. *J. Am. Chem. Soc.* **2009**, *131*, 5930–5934.
(31) Collin, J.-P.; Kayhanian, R.; Sauvage, J.-P.; Calogero, G.; Barigelletti, F.; De Cian, A.; Fischer, J. *Chem. Commun.* **1997**, 775–776.
(32) Alonso-Vante, N.; Nierengarten, J.-F.; Sauvage, J.-P. *J. Chem. Soc., Dalton Trans.* **1994**, 1649–1654.
(33) Beley, M.; Chodorowski, S.; Collin, J.-P.; Sauvage, J.-P.; Flamigni, L.; Barigelletti, F. *Inorg. Chem.* **1994**, *33*, 2543–2547.
(34) Wadman, S. H.; Lutz, M.; Tooke, D. M.; Spek, A. L.; Hartl, F.; Havenith, R. W. A.; van Klink, G. P. M.; van Koten, G. *Inorg. Chem.* **2009**, *48*, 1887–1900.
(35) Bomben, P. G.; Robson, K. C. D.; Sedach, P. A.; Berlinguette, C. P. *Inorg. Chem.* **2009**, *48*, 9631–9643.
(36) Koivisto, B. D.; Robson, K. C. D.; Berlinguette, C. P. *Inorg. Chem.* **2009**, *48*, 9644–9652.
(37) Lo, S. C.; Namdas, E. B.; Burn, P. L.; Samuel, I. D. W. *Macromolecules* **2003**, *36*, 9721–9730.

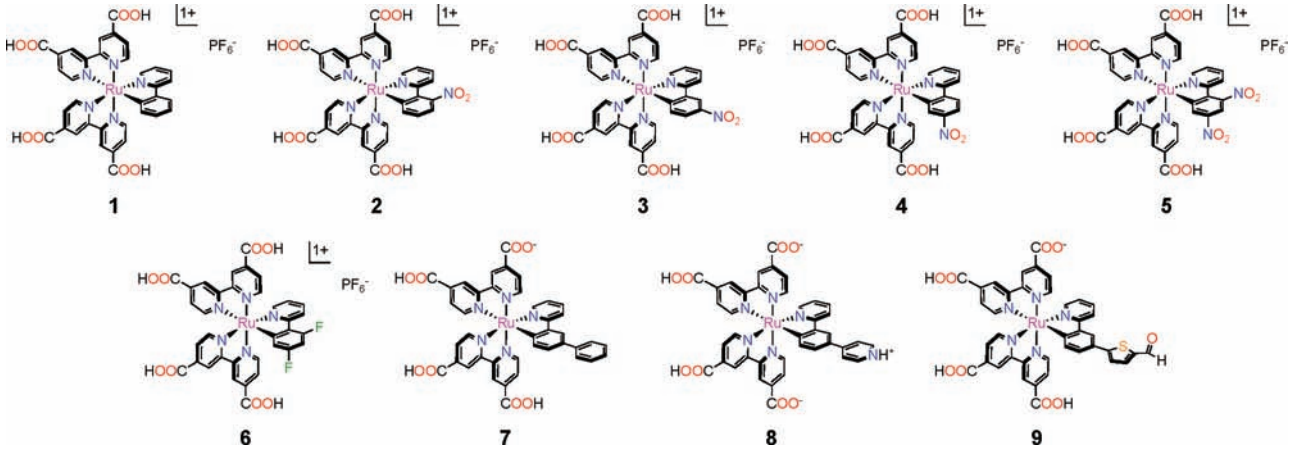

Figure 2. Cyclometalated Ru(II) complexes **1**−**9** under investigation in this study.

Chart 1. Designation of Compounds[a]

$[Ru(dcbpyH_2)_2(\mathbf{L1})]PF_6$	**1**
$(Bu_4N)_3[Ru(dcbpy)(dcbpyH)(\mathbf{L1})]PF_6$	**1a**
$[Ru(dcbpyH_2)_2(\mathbf{L2})]PF_6$	**2**
$[Ru(dcbpyH_2)_2(\mathbf{L3})]PF_6$	**3**
$(Bu_4N)_4[Ru(dcbpy)_2(\mathbf{L3})]PF_6$	**3a**
$[Ru(dcbpyH_2)_2(\mathbf{L4})]PF_6$	**4**
$[Ru(dcbpyH_2)_2(\mathbf{L5})]PF_6$	**5**
$[Ru(dcbpyH_2)_2(\mathbf{L6})]PF_6$	**6**[30]
$(Bu_4N)_3[Ru(dcbpy)(dcbpyH)(\mathbf{L6})]PF_6$	**6a**
$[Ru(dcbpyH_2)(dcbpyH)(\mathbf{L7})]$	**7**
$(Bu_4N)_3[Ru(dcbpy)_2(\mathbf{L7})]$	**7a**
$[Ru(dcbpyH)_2(\mathbf{L8}\text{-H})]$	**8**
$(Bu_4N)_3[Ru(dcbpy)_2(\mathbf{L8})]$	**8a**
$[Ru(dcbpyH_2)(dcbpyH)(\mathbf{L9})]$	**9**
$(Bu_4N)_3[Ru(dcbpy)_2(\mathbf{L9})]$	**9a**

[a] $dcbpyH_2$ = 4,4′-dicarboxy-2,2′-bipyridine (dcbpyH and dcbpy indicate monoanionic and dianionic forms of $dcbpyH_2$, respectively); **HL1** = 2-phenylpyridine; **HL2** = 2-(2-nitrophenyl)pyridine; **HL3** = 2-(3-nitrophenyl)pyridine; **HL4** = 2-(4-nitrophenyl)pyridine; **HL5** = 2-(2,4-dinitrophenyl)pyridine; **HL6** = 2-(2,4-difluorophenyl)pyridine; **HL7** = 2-(biphenyl-3-yl)pyridine; **HL8** = 2,4′-(1,3-phenylene)dipyridine; **HL9** = 5-(3-(pyridin-2-yl)phenyl)thiophene-2-carbaldehyde.

2-(3-bromophenyl)pyridine[38] was cooled to −78 °C. To this solution was added 1 mL portions of *n*-BuLi (1.6 M in hexanes, 5.1 mL, 13 mmol) resulting in a dark green solution. After 45 min of stirring at −78 °C, 3.0 g (16 mmol) of 2-isopropoxy-4,4,5,5-tetramethyl-1,3,2-dioxaborolane was added and stirred at −78 °C for 30 min. The dry ice bath was then removed, and the reaction was left to warm to room temperature overnight. The reaction was then quenched with MeOH (5 mL), preabsorbed on silica, and the solvent was removed in vacuo. The sample was purified using chromatography [SiO_2: (DCM/EtOAc 9:1): R_f = 0.57] to afford 2.2 g (73%) of a colorless oil. ^{1}H NMR (400 MHz, $CDCl_3$): δ = 8.67 (ddd, ^3J = 5 Hz, ^4J = 2 Hz, ^5J = 1 Hz, 1H, H_a), 8.37 (s, 1H, H_e), 8.11 (ddd, ^3J = 8 Hz, ^4J = 2 Hz, ^5J = 1 Hz, 1H, H_f), 7.84 (dt, ^3J = 8 Hz, ^4J = 1 Hz, 1H, H_h), 7.77 (dt, ^3J = 8 Hz, ^4J = 1 Hz, 1H, H_d), 7.71 (dt, ^3J = 7 Hz, ^4J = 2 Hz, 1H, H_c), 7.47 (t, ^3J = 8 Hz, 1H, H_g), 7.19 (ddd, ^3J = 7 Hz, ^4J = 5 Hz, ^5J = 1 Hz, 1H, H_b), 1.34 (s, 12H, H_{Methyl}); ^{13}C NMR (100 MHz, $CDCl_3$): δ = 157.7, 149.8, 139.0, 136.8, 135.5, 133.4, 130.0, 128.4, 122.2, 120.9, 84.1, 25.1; HRMS (EI): m/z = 281.1598 [$(M)^+$] (calcd for $C_{17}H_{20}BNO_2^+$: m/z = 281.1587).

2-(2-Nitrophenyl)pyridine (HL2). An alternative method to a previously reported synthesis is provided.[39] A THF (30 mL) solution containing 500 mg (2.48 mmol) of 1-bromo-2-nitrobenzene was charged with 5.0 mL (2.5 mmol) of a 0.5 M THF solution containing 2-pyridylzinc bromide. This mixture was stirred for 5 min prior to the addition of 143 mg (0.124 mmol) of $Pd(PPh_3)_4$, and then heated at reflux for 15 h. The resultant solution was filtered to obtain a brown filtrate that formed a brown/orange solid upon removal of solvent in vacuo. Purification by column chromatography [SiO_2: (hexanes/EtOAc 5:2)] afforded 265 mg (53.5%) of the product as a yellow oil that solidified upon standing overnight at 4 °C. ^{1}H NMR ($CDCl_3$): δ 8.66 (ddd, ^3J = 5 Hz, ^4J = 1 Hz, ^5J = 1 Hz, 1H, H_a), 7.90 (dd, ^3J = 8 Hz, ^4J = 1 Hz, 1H, H_h), 7.80 (td, ^3J = 8 Hz, ^4J = 2 Hz, 1H, H_c), 7.65 (m, 2H, H_e, H_f), 7.55 (ddd, ^3J = 9 Hz, 7 Hz, ^4J = 2 Hz, 1H, H_g), 7.48 (dt, ^3J = 8 Hz, ^4J = 1 Hz, ^5J = 1 Hz, 1H, H_d), 7.33 (ddd, ^3J = 8 Hz, 5 Hz, ^4J = 1 Hz, 1H, H_b). EI-MS: m/z 199.9 (calcd for $C_{11}H_8N_2O_2^+$: m/z 200.0).

2-(3-Nitrophenyl)pyridine (HL3). An alternative method to a previously reported synthesis is provided.[40] A THF/EtOH (20 mL) solution (THF:EtOH, 3:1 v:v) containing 501 mg (3.00 mmol) of 3-nitrophenylboronic acid, 966 mg (7.00 mmol) of K_2CO_3 and 173 mg (0.150 mmol) of $Pd(PPh_3)_4$ was charged with 0.26 mL (2.7 mmol) of 2-bromopyridine and then heated at reflux for 65 h. The suspension was then filtered to obtain an orange filtrate that afforded a dark red-orange oil upon removal of solvent in vacuo. Purification by column chromatography [SiO_2: (hexanes/EtOAc/$CHCl_3$ 5:2:3)] yields a light yellow solid that was recrystallized from EtOH affording 465 mg (87.2%) of the product as a pale yellow crystalline solid. ^{1}H NMR ($CDCl_3$): δ 8.87 (dd, ^4J = 2 Hz, 2 Hz, 1H, H_h), 8.75 (ddd, ^3J = 8 Hz, ^4J = 2 Hz, ^5J = 1 Hz, 1H, H_a), 8.38 (ddd, ^3J = 8 Hz, ^4J = 2 Hz, 1 Hz,

(38) van der Sluis, M.; Beverwijk, V.; Termaten, A.; Bickelhaupt, F.; Kooijman, H.; Spek, A. L. *Organometallics* **1999**, *18*, 1402–1407.

(39) Molina, P.; Lorenzo, A.; Aller, E. *Tetrahedron* **1992**, *48*, 4601–4616.

(40) Bullock, D. J. W.; Cumper, C. W. N.; Vogel, A. I. *J. Chem. Soc.* **1965**, 5311–5316.

1H, H_g), 8.28 (ddd, ^3J = 8 Hz, ^4J = 2 Hz, 1 Hz, 1H, H_e), 7.83 (m, 2H, H_c, H_d), 7.66 (dd, ^3J = 8 Hz, 8 Hz, 1H, H_f), 7.34 (ddd, 1H, H_b). EI-MS: m/z 200 (calcd for $C_{11}H_8N_2O_2^+$: m/z 200.0).

2-(4-Nitrophenyl)pyridine (HL4). An alternative to a previously reported synthesis is provided.[41] A THF (25 mL) solution containing 503 mg (2.49 mmol) of 4-bromo-2-nitrobenzene was charged with 5.0 mL (2.5 mmol) of a 0.5 M THF solution of 2-pyridylzinc bromide and stirred for 5 min prior to the addition of 143 mg (0.124 mmol) of $Pd(PPh_3)_4$. The solution was heated at reflux for 16 h, and then filtered to obtain an orange/brown filtrate. The organic layer was washed with H_2O (3 × 15 mL), collected, and the solvent removed in vacuo resulting in a white solid that was purified by column chromatography [SiO_2: (hexanes/EtOAc/$CHCl_3$ 5:2:3)] to afford 276 mg (55.4%) of the product as a white solid. ^{1}H NMR ($CDCl_3$): δ 8.76 (dt, ^3J = 5 Hz, ^4J = 1 Hz, ^5J = 1 Hz, 1H, H_a), 8.34 (dt, ^3J = 9 Hz, ^4J = 2 Hz, ^5J = 2 Hz, 2H, H_f), 8.19 (dt, ^3J = 9 Hz, ^4J = 2 Hz, ^5J = 2 Hz, 2H, H_e), 7.87−7.82 (m, 2H, H_c, H_d), 7.35 (ddd, ^3J = 7 Hz, 5 Hz, ^4J = 2 Hz, 1H, H_b). EI-MS: m/z 199.9 (calcd for $C_{11}H_8N_2O_2^+$: m/z 200.0).

2-(2,4-Dinitrophenyl)pyridine (HL5). A THF (25 mL) solution containing 1.012 mg (4.097 mmol) of 1-bromo-2,4-dinitrobenzene was charged with 8.3 mL (4.2 mmol) of a 0.5 M THF solution containing 2-pyridylzinc bromide and stirred for 5 min prior to the addition of 240 mg (0.208 mmol) of $Pd(PPh_3)_4$. The solution was heated at reflux for 17 h, and then filtered to obtain a brown filtrate. Subsequent solvent removal in vacuo left a dark orange/brown oil that was purified by column chromatography [SiO_2: (hexanes/EtOAc/$CHCl_3$ 5:2:3)] to afford 604 mg (60.2%) of the product as a yellow oil that solidified upon standing overnight at 4 °C. ^{1}H NMR ($CDCl_3$): δ 8.74 (d, ^4J = 2 Hz, 1H, H_g), 8.70 (ddd, ^3J = 5 Hz, ^4J = 1 Hz, ^5J = 1 Hz, 1H, H_a), 8.51 (dd, ^3J = 8 Hz, ^4J = 2 Hz, 1H, H_f), 7.87 (m, 2H, H_c, H_e), 7.55 (dt, ^3J = 8 Hz, ^4J = 1 Hz, ^5J = 1 Hz, 1H, H_d), 7.41 (ddd, ^3J = 8 Hz, 5 Hz, ^4J = 1 Hz, 1H, H_b). ^{13}C NMR ($CDCl_3$): 153.4, 150.4, 149.5, 147.7, 140.8, 137.4, 132.7, 126.8, 124.2, 123.0, 120.2. HRMS (EI): m/z 245.0444 [(M^+)] (calcd for $C_{11}H_7N_3O_4^+$: m/z 245.0437).

2-(Biphenyl-3-yl)pyridine (HL7). A sparged mixture of THF (45 mL) and H_2O (5 mL) containing 0.69 g (3.0 mmol) of 2-(3-bromophenyl)pyridine[38] and 400 mg (3.28 mmol) of phenylboronic acid was charged with 2.27 g (16.4 mmol) of K_2CO_3 and 265 mg (0.229 mmol) of $Pd(PPh_3)_4$. The suspension was heated at reflux for 14 h under an inert atmosphere, then cooled and poured into H_2O. The product was extracted with diethyl ether, washed with brine, and then dried with $MgSO_4$. Filtration and removal of the solvent in vacuo resulted in an oil that was purified by column chromatography [basic Al_2O_3: DCM/hexane 1:1; R_f = 0.78] affording 650 mg (95.2%) of the product as a colorless oil. ^{1}H NMR (400 MHz, $CDCl_3$): δ = 8.78 (ddd, ^3J = 5 Hz, ^4J = 2 Hz, ^5J = 1 Hz, 1H, H_a), 8.32 (t, ^4J = 2 Hz, 1H, H_e), 8.03 (dt, ^3J = 8 Hz, ^4J = 2 Hz, ^5J = 1 Hz, 1H, H_f), 7.85−7.67 (m, 5H, H_d, H_h, H_c, H_i), 7.59 (t, ^3J = 8 Hz, 1H, H_g), 7.51 (t, ^3J = 7 Hz, 2H, H_j), 7.42 (t, ^3J = 7 Hz, 1H, H_k), 7.28 (ddd, ^3J = 7 Hz, ^4J = 5 Hz, ^5J = 1 Hz, 1H, H_b); ^{13}C NMR (100 MHz, $CDCl_3$): δ =157.1, 149.4, 141.7, 140.9, 139.6, 136.9, 129.2, 128.8, 127.8, 127.4, 127.2, 125.8, 122.2, 120.6; HRMS (EI): m/z = 231.1042 [$(M)^+$] (calcd for $C_{17}H_{13}N^+$: m/z = 231.1048).

2,4′-(1,3-Phenylene)dipyridine (HL8). A sparged mixture of THF (45 mL) and H_2O (5 mL) containing 330 mg (1.17 mmol) of 2-(3-(4,4,5,5-tetramethyl-1,3,2-dioxaborolan-2-yl)phenyl)pyridine[37] and 251 mg (1.29 mmol) of 4-bromopyridine was charged with 811 mg (5.88 mmol) of K_2CO_3 and 95 mg (0.082 mmol) of $Pd(PPh_3)_4$. The suspension was heated at reflux for 14 h under inert atmosphere. The reaction mixture was then cooled and poured into H_2O. The product was extracted with diethyl ether, washed with brine, and then dried with $MgSO_4$. Filtration and removal of the solvent in vacuo resulted in an oil that was purified using column chromatography [SiO_2: using a gradient DCM/EtOAc 8:2 to remove impurities and then increasing to the more polar DCM/EtOAc/MeOH 8:1:1] to afford 200 mg (73%) of the product as a colorless oil. ^{1}H NMR (400 MHz, $CDCl_3$): δ = 8.63 (d, ^3J = 5 Hz, 1H, H_a), 8.58 (d, ^3J = 6 Hz, 2H, H_j), 8.23 (s, 1H, H_e), 7.94 (d, ^3J = 8 Hz, 1H, H_f), 7.70−7.64 (m, 2H, H_d, H_c), 7.57 (d, ^3J = 8 Hz, 1H, H_h), 7.50−7.45 (m, 3H, H_i, H_g), 7.16 (ddd, ^3J = 7 Hz, ^4J = 5 Hz, ^5J = 1 Hz, 1H, H_b). ^{13}C NMR (100 MHz, $CDCl_3$): δ = 156.5, 150.1, 149.6, 148.1, 140.1, 138.4, 136.8, 129.4, 127.4, 127.3, 125.5, 122.4, 121.6, 120.5. HRMS (EI): m/z = 232.1007 [$(M)^+$] (calcd for $C_{16}H_{12}N_2^+$: m/z = 232.1000).

5-(3-(Pyridin-2-yl)phenyl)thiophene-2-carbaldehyde (HL9). A sparged mixture of THF (45 mL) and H_2O (5 mL) containing 1.10 g (3.91 mmol) of 2-(3-(4,4,5,5-tetramethyl-1,3,2-dioxaborolan-2-yl)phenyl)pyridine[37] and 747 mg (3.91 mmol) of 5-bromothiophene-2-carbaldehyde was charged with 2.70 g (19.6 mmol) of K_2CO_3 and 316 mg (0.273 mmol) of $Pd(PPh_3)_4$. The mixture was heated at reflux for 14 h under inert atmosphere, then cooled and poured into H_2O. The product was extracted with diethyl ether, washed with brine and dried with $MgSO_4$. Filtration and removal of the solvent in vacuo resulted in an oil that was purified by column chromatography [SiO_2: (DCM/EtOAc 9:1): R_f = 0.57] to afford 820 mg (79.0%) of the product, an oil that solidified as a yellow solid upon standing. ^{1}H NMR (400 MHz, $CDCl_3$): δ = 9.87 (s, 1H, H_k), 8.70 (ddd, ^3J = 5 Hz, ^4J = 2 Hz, ^5J = 1 Hz, 1H, H_a), 8.31 (t, ^4J = 2 Hz, 1H, H_e), 7.95 (ddd, ^3J = 8 Hz, ^4J = 2 Hz, ^5J = 1 Hz, 1H, H_f), 7.83−7.75 (m, 3H, H_c, H_h, H_j), 7.67 (dt, ^3J = 8 Hz, ^4J = 1 Hz, 1H, H_d), 7.50 (t, ^3J = 8 Hz, 1H, H_g), 7.47 (d, ^3J = 8 Hz, 1H, H_i), 7.25 (ddd, ^3J = 7 Hz, ^4J = 5 Hz, ^5J = 1 Hz, 1H, H_b); ^{13}C NMR (100 MHz, $CDCl_3$): δ = 183.0, 156.6, 154.2, 150.0, 142.8, 140.6, 137.5, 137.1, 133.8, 129.8, 128.0, 127.0, 125.2, 124.7, 122.8, 120.8; HRMS (EI): m/z = 265.0548 [$(M)^+$] (calcd for $C_{16}H_{11}NOS^+$: m/z = 265.0561).

General Synthetic Procedure for Precursors P1−P9. The addition of **HL1**−**HL9** to the Ru precursor, [(η^6-*p*-cymene)$RuCl_2$]$_2$, leads to a mixture of [$Ru(CH_3CN)_4$(**L#**)]PF_6 and [Ru(*p*-cymene)$(CH_3CN)_2$(**L#**)]PF_6 (denoted **P#**; Scheme 1). While it is possible to isolate each of these cyclometalated Ru species, they both serve as satisfactory precursors to the target metal complexes **1**−**9**. We therefore did not attempt to isolate each of these intermediates; while experimental data for most mixtures is not provided, representative characterization data for **P1** and **P5** is included. *General synthetic protocol*: A flask containing 0.33 mmol of [(η^6-*p*-cymene)$RuCl_2$]$_2$, 0.66 mmol of **HL#**, 0.66 mmol of NaOH and 1.32 mmol of KPF_6 in 5 mL of MeCN was stirred at 45 °C for 2 days (Scheme 1). The resultant reaction mixture was filtered to remove the suspended solid. The solvent was then removed in vacuo, and reconstituted in a minimum volume of a 9:1 CH_2Cl_2/MeCN solvent mixture and purified by column chromatography [basic Al_2O_3: (CH_2Cl_2/MeCN 9:1)]. The yellow/orange band was collected, and the solvent was removed. The crude product was precipitated using CH_2Cl_2/diethyl ether, filtered, and washed with diethyl ether to afford the desired mixture **P#**. The mixture was verified by ^{1}H NMR spectroscopy, and used as prepared in subsequent reactions without further separation or purification.

[Ru(*p*-cymene)$(CH_3CN)_2$(L1)]PF_6 (P1). An MeCN (5 mL) suspension containing 101 mg (0.653 mmol) of **HL1**, 26 mg (0.65 mmol) of crushed NaOH, 241 mg (1.31 mmol) of KPF_6 and 199 mg (0.325 mmol) of [(η^6-p-cymene)$RuCl_2$]$_2$ was stirred at 45 °C for 2 days. The reaction mixture was then cooled and filtered to remove suspended solid, followed by the removal of solvent in vacuo to yield an orange/brown solid. The solid was purified by column chromatography [basic Al_2O_3: (CH_2Cl_2/MeCN 9:1)]. The yellow fraction that was collected and reconstituted in a minimum volume of CH_2Cl_2, and was then drawn out of solution with diethyl ether. The resultant solid was

(41) Walla, P.; Kappe, C. O. *Chem. Commun.* **2004**, 564–565.

Scheme 1. General Synthetic Scheme Illustrating the Initial Cyclometalation of $[(\eta^6\text{-}p\text{-cymene})RuCl_2]_2$ with **HL1**−**HL9** to Form a Mixture of Intermediates **P1**−**P9** (Denoted by Dashed Box), which Render Complexes **1**−**9** upon Coordination with 2 equiv of $dcbpyH_2$[a]

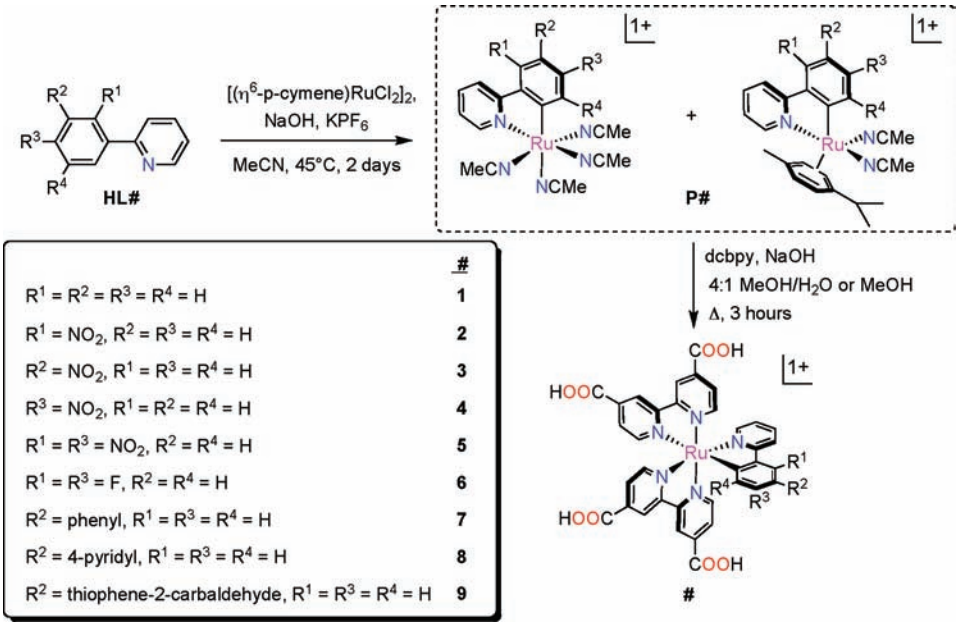

[a] Protonation levels vary for certain complexes; see Chart 1 for precise formulations.

filtered, washed with diethyl ether (3 × 10 mL), and dried to afford 280 mg (69.9%) of the product as a yellow/green solid. ^{1}H NMR (CD_3CN): δ 9.20 (td, ^3J = 6 Hz, ^4J = 1 Hz, 1H), 8.14 (dd, ^3J = 8 Hz, ^4J = 1 Hz, 1H), 7.91 (m, 2H), 7.76 (dd, ^3J = 8 Hz, ^4J = 1 Hz, 1H), 7.25 (m, 2H), 7.15 (dt, ^3J = 8 Hz, ^4J = 1 Hz, 1H) 5.93 (d, ^3J = 6 Hz, 2H), 5.65 (dd, ^3J = 6 Hz, ^4J = 1 Hz, 1H), 5.41 (dd, ^3J = 6 Hz, ^4J = 1 Hz, 1H), 2.35 (septet, ^3J = 7 Hz, 1H), 2.12 (s, 3H), 2.04 (s, 3H), 1.99 (s, 3H), 0.93 (d, ^3J = 7 Hz, 3H), 0.91 (d, ^3J = 7 Hz, 3H). ^{13}C NMR (CD_3CN): 176.0, 166.6, 156.8, 145.5, 141.1, 139.7, 130.7, 125.4, 124.8, 123.7, 120.5, 105.0, 103.3, 93.4, 89.3, 85.7, 31.9, 22.5, 22.3, 18.9, 3.9.

[Ru(CH$_3$CN)$_4$(L5)]PF$_6$ (P5). An MeCN (5 mL) suspension containing 161 mg (0.657 mmol) of **HL5**, 26 mg (0.65 mmol) of crushed NaOH, 241 mg (1.30 mmol) of KPF_6 and 200 mg (0.327 mmol) of $[(\eta^6\text{-p-cymene})RuCl_2]_2$ was refluxed for 2 days and then filtered to yield a deep purple solution. Solvent was removed in vacuo, and the resultant solid was reconstituted in a minimum volume of 9:1 CH_2Cl_2/MeCN and purified by column chromatography [basic Al_2O_3: (CH_2Cl_2/MeCN 9:1)]. After the solvent was removed in vacuo, the residual solid was dissolved in a minimal volume of MeCN and drawn out of solution by the slow addition of diethyl ether. The solid was isolated and washed with diethyl ether (3 × 10 mL) to afford 144 mg (34.2%) of a pink solid product. ^{1}H NMR (CD_3CN): δ 9.13 (ddd, ^3J = 6 Hz, ^4J = 2 Hz, ^5J = 1 Hz, 1H), 8.90 (d, ^4J = 2 Hz, 1H), 7.92 (d, ^4J = 2 Hz, 1H), 7.83 (ddd, ^3J = 9 Hz, 8 Hz, ^4J = 2 Hz, 1H), 7.52 (dt, ^3J = 8 Hz, ^4J = 1 Hz, 1H), 7.38 (ddd, ^3J = 7 Hz, 6 Hz, ^4J = 1 Hz, 1H), 2.57 (s, 3H), 2.02 (s, 6H), 1.97 (s, 3H). ^{13}C NMR (CD_3CN): 197.2, 162.4, 155.0, 148.6, 145.8, 142.4, 138.1, 134.2, 125.3, 125.2, 123.1, 123.0, 112.2, 4.5, 4.0.

General Synthetic Procedure for 1−4, 6. A degassed aqueous MeOH solution (5 mL; H_2O/MeOH, 1:4 v:v) containing 0.20 mmol of $dcbpyH_2$ and 0.40 mmol of crushed NaOH was stirred for 40 min prior to the addition of 0.10 mmol of **P#.** The solution was brought to reflux for 3 h, cooled to room temperature, followed by the removal of solvent in vacuo. The resultant dark purple solid was reconstituted in H_2O, followed by the dropwise addition of 0.2 M HPF_6 until the formation of a precipitate was observed. The isolated precipitate was washed with H_2O (3 × 10 mL), reconstituted in DMF, and then drawn out of solution with diethyl ether. The solid was collected by filtration, washed with diethyl ether (3 × 10 mL), and dried in air.

[Ru(dcbpyH$_2$)$_2$(L1)]PF$_6$ (1). Yield: 55 mg (61%) of the product as a dark purple solid. Characterization data matches the previously reported synthesis.[35]

[Ru(dcbpyH$_2$)$_2$(L2)]PF$_6$ (2). Yield: 93 mg (77%) of the product as a dark purple solid. ^{1}H NMR (CD_3OD with a drop of NaOD): δ 9.11 (s, 1H), 9.04 (s, 1H), 8.98 (s, 2H), 8.22 (dd, ^3J = 6 Hz, ^4J = 1 Hz, 1H), 7.94 (m, 4H), 7.75 (m, 5H), 7.58 (d, ^3J = 8 Hz, 1H), 7.07 (m, 2H), 6.95 (t, ^3J = 8 Hz, 1H), 6.61 (dd, ^3J = 8 Hz, ^4J = 1 Hz, 1H). ESI-MS: m/z 789.02 (calcd for $RuC_{35}H_{23}N_6O_{10}$ 789.05). Anal. Calcd. for $RuC_{35}H_{23}N_6O_{10}PF_6$: C, 45.03; H, 2.48; N, 9.00. Found: C, 45.43, H, 2.77, N, 9.37.

[Ru(dcbpyH$_2$)$_2$(L3)]PF$_6$ (3). Yield: 178 mg (87.4%) of the product as a dark purple solid. ^{1}H NMR (CD_3OD): δ 9.04 (s, 1H), 8.96 (s, 1H), 8.92 (s, 1H), 8.90 (s, 1H), 8.68 (d, ^4J = 2 Hz, 1H), 8.27 (d, ^3J = 8 Hz, 1H), 7.99 (d, ^3J = 6 Hz, 1H), 7.92−7.88 (m, 2H), 7.85−7.75 (m, 3H), 7.70 (dd, ^3J = 6 Hz, ^4J = 2 Hz, 1H), 7.68−7.56 (m, 3H), 7.50 (d, ^3J = 6 Hz, 1H), 7.10 (ddd, ^3J = 7 Hz, 6 Hz, ^4J = 1 Hz 1H), 6.74 (d, ^3J = 8 Hz, 1H). HRMS (MALDI-TOF): m/z 789.0492 [M^+] (calcd for $C_{35}H_{23}N_6O_{10}Ru^+$: m/z 789.0523). Anal. Calcd. for $RuC_{35}H_{23}N_6O_{10}PF_6$ + $7H_2O$: C, 39.67; H, 3.52; N, 7.93. Found: C, 39.74; H, 3.19; N, 7.92.

[Ru(dcbpyH$_2$)$_2$(L4)]PF$_6$ (4). Yield: 132 mg (99.0%) of the product as a dark purple solid. ^{1}H NMR (CD_3OD with a drop of NaOD): δ 9.03 (s, 1H), 8.96 (s, 1H), 8.95 (s, 1H), 8.90 (s, 1H), 8.26 (d, ^3J = 8 Hz, 1H), 8.08 (d, ^3J = 9 Hz, 1H), 8.03 (d, ^3J = 6 Hz, 1H), 7.76 (m, 10H), 7.23 (d, ^4J = 2 Hz, 1H), 7.13 (dd, ^3J = 8 Hz, ^4J = 1 Hz, 1H). ^{13}C NMR (CD_3OD with a drop of NaOD): 195.8, 171.2, 171.1, 171.0, 170.9, 170.7, 166.8, 159.3, 158.5, 158.3, 157.0, 155.4, 153.8, 151.9, 151.3, 151.2, 150.3, 148.7, 147.9, 146.6, 145.7, 145.6, 137.7, 129.6, 127.8, 127.4, 126.9, 126.8, 125.5, 124.2, 124.1, 124.0, 123.8, 122.2, 117.5. HRMS (ESI): m/z = 789.05200 [M^+] (calcd for [$RuC_{35}H_{23}N_6O_{10}]^+$: m/z = 783.05196). Anal. Calcd. for $RuC_{35}H_{23}N_6O_{10}PF_6$ + DMF + $2H_2O$: C, 50.84; H, 3.82; N, 10.92. Found: C, 50.63; H,3.91; N, 10.83.

[Ru(dcbpyH$_2$)$_2$(L5)]PF$_6$ (5). A degassed aqueous methanol solution (5 mL; H_2O/MeOH, 1:4 v:v) containing 22 mg

(0.092 mmol) of $dcbpyH_2$ and 7 mg (0.2 mmol) of crushed NaOH was stirred for 40 min prior to the addition of 30 mg (0.046 mmol) of **P5**. The light purple solution was brought to reflux for 3 h and then cooled to room temperature. Removal of solvent in vacuo yielded a dark purple solid that was purified by column chromatography [SiO_2: (12 cm ×2 cm)($MeOH/CHCl_3$ 3:1)]. The purple band was collected followed by the removal of solvent in vacuo. The resultant solid was dissolved in a minimum volume of MeOH and drawn out of solution with acetone. The solid was collected by filtration and washed with diethyl ether (3 × 10 mL). The solid was reconstituted in H_2O, followed by the dropwise addition of 0.2 M HPF_6 until the formation of a precipitate was observed. The solid was collected by filtration, washed with H_2O (3 × 10 mL), and then reconstituted in DMF and drawn out of solution with diethyl ether. The solid was isolated, washed with diethyl ether (3 × 10 mL), and dried to afford 25 mg (56%) of the product as a dark purple solid. ^{1}H NMR (CD_3OD with a drop of NaOD): δ 9.05 (s, 1H), 8.98 (s, 2H), 8.94 (s, 1H), 8.02 (d, ^3J = 6 Hz, 1H), 7.75 (m, 11H), 7.47 (d, ^4J = 2 Hz, 1H), 7.19 (ddd, ^3J = 7 Hz, 6 Hz, ^4J = 1 Hz, 1H). ^{13}C NMR (D_2O with a drop of NaOD and MeOD): 202.5, 172.7, 172.6, 172.4, 172.2, 169.5, 161.1, 158.8, 157.9, 157.8, 156.3, 155.6, 152.8, 151.9, 151.6, 150.5, 148.5, 145.8, 145.6, 144.6, 144.1, 144.0, 142.2, 137.3, 132.1, 127.0, 126.9, 126.5, 126.4, 126.2, 124.3, 123.7, 123.6, 123.5, 112.5. ESI-MS: m/z 833.95 [M^+] (calcd for $RuC_{35}H_{22}N_7O_{12}$ 834.04). Anal. Calcd. for $RuC_{35}H_{23}N_6O_{10}PF_6 + 2CH_3OH$: C, 42.62; H, 2.90; N, 9.40. Found: C, 43.02; H,3.18; N, 9.66.

[Ru(dcbpyH$_2$)$_2$(L6)]PF$_6$ (6). Yield: 109 mg (87.5%) of the product as a dark purple solid. All characterization data matches the previously reported synthesis.[30]

[Ru(dcbpyH$_2$)(dcbpyH)(L7)] (7). A degassed aqueous methanol (15 mL) solution (H_2O/MeOH, 1:4 v:v) containing 194 mg (0.794 mmol) of $dcbpyH_2$ and 64 mg (1.6 mmol) of crushed NaOH was stirred for 40 min prior to the addition of 261 mg (0.401 mmol) of **P7.** The reaction mixture was brought to reflux for 3 h generating a color change from yellow/green to dark purple. Insoluble particulates were removed from the solution by filtration, followed by the removal of solvent from the filtrate in vacuo. Further purification by column chromatography [SiO_2: ($MeOH/CHCl_3$ 3:1) followed by Sephadex LH-20: (D_2O)] yielded the deprotonated product as a sodium salt. The solid was reconstituted in H_2O, followed by the addition of 0.2 M HNO_3 until the formation of a precipitate was observed and placed in the refrigerator overnight. The solid was isolated by filtration, washed with acid (pH 3) and dried in vacuo to afford 51 mg (14%) of the dark purple product. ^{1}H NMR (CD_3OD with a drop of NaOD): δ 9.03 (s, 1H), 8.95 (s, 1H), 8.91 (s, 1H), 8.88 (s, 1H), 8.22 (dd, ^3J = 6 Hz, ^4J = 2 Hz, 1H), 8.19 (d, ^3J = 8 Hz, 1H), 8.11 (d, ^3J = 2 Hz, 1H), 7.94 (dd, ^3J = 6 Hz, ^4J = 1 Hz, 1H), 7.87 (dd, ^3J = 6 Hz, ^4J = 1 Hz, 1H), 7.86 (dd, ^3J = 6 Hz, ^4J = 2 Hz, 1H), 7.83 (dd, ^3J = 6 Hz, ^4J = 1 Hz, 1H), 7.73 (ddd, ^3J = 9 Hz, 7 Hz, ^4J = 2 Hz, 1H), 7.68 (dd, ^3J = 6 Hz, ^4J = 2 Hz, 1H), 7.65−7.60 (m, 4H), 7.56 (ddd, ^3J = 6 Hz, ^4J = 2 Hz, ^5J = 1 Hz, 1H), 7.37 (t, ^3J = 7 Hz, 2H), 7.23 (t, ^3J = 7 Hz, 1H), 7.12 (dd, ^3J = 8 Hz, ^4J = 2 Hz, 1H), 6.98 (ddd, ^3J = 7 Hz, 6 Hz, ^4J = 1 Hz, 1H), 6.51 (d, ^3J = 8 Hz, 1H). Anal. Calcd. for $RuC_{41}H_{27}N_5O_8 + 2H_2O$: C, 57.61; H, 3.66; N, 8.19. Found: C, 57.29; H, 3.72; N, 8.04.

[Ru(dcbpyH)$_2$(L8-H)] (8). A degassed H_2O/MeOH (15 mL) solution (H_2O/MeOH, 1:4 v:v) containing 218 mg (0.892 mmol) of $dcbpyH_2$ and 72 mg (1.8 mmol) of crushed NaOH was stirred for 40 min prior to the addition of 287 mg (0.440 mmol) of **P8.** The solution was brought to reflux for 3 h leading to a color change from yellow to dark purple. A reaction workup analogous to that of **7** affords 26 mg (6%) of a dark purple product. ^{1}H NMR (CD_3OD with a drop of NaOD): δ 9.04 (s, 1H), 8.95 (s, 1H), 8.91 (s, 1H), 8.89 (s, 1H), 8.49 (dd, ^3J = 5 Hz, ^4J = 2 Hz, 2H), 8.28 (m, 2H), 8.17 (dd, ^3J = 6 Hz, ^4J = 1 Hz, 1H), 7.93 (dd, ^3J = 6 Hz, ^4J = 1 Hz, 1H), 7.87 (dd, ^3J = 6 Hz, ^4J = 2 Hz, 1H), 7.85 (dd, ^3J = 6 Hz, ^4J = 1 Hz, 1H), 7.82 (dd, ^3J = 6 Hz, ^4J = 1 Hz, 1H), 7.78 (ddd, ^3J = 9 Hz, 8 Hz, ^4J = 2 Hz, 1H), 7.75 (dd, ^3J = 5 Hz, ^4J = 2 Hz, 2H), 7.69 (dd, ^3J = 6 Hz, ^4J = 2 Hz, 1H), 7.66 (dd, ^3J = 6 Hz, ^4J = 2 Hz, 1H), 7.61 (m, 2H), 7.24 (dd, ^3J = 8 Hz, ^4J = 2 Hz, 1H), 7.03 (ddd, ^3J = 7 Hz, 6 Hz, ^4J = 1 Hz, 1H), 6.63 (d, ^3J = 8 Hz, 1H). ^{13}C NMR (CD_3OD with a drop of NaOD): 198.9, 171.4, 171.3, 171.1, 171.0, 168.4, 159.4, 158.7, 158.3, 156.9, 155.3, 151.8, 151.4, 151.2, 151.0, 150.4, 150.1, 148.0, 147.7, 146.4, 145.3, 145.1, 137.5, 137.4, 131.5, 127.8, 127.6, 127.1, 126.7, 126.6, 124.1, 124.0, 123.7, 123.6, 123.0, 122.4, 120.7. HRMS (MALDI-TOF): m/z = 821.0962 [M^+] (calcd for $[RuC_{40}H_{28}N_6O_8]^+$: m/z = 821.0939). Anal. Calcd. for $RuC_{40}H_{28}N_6O_8 + 3H_2O$: C, 53.87; H, 3.84; N, 9.43. Found: C, 53.61; H, 3.26; N, 9.42.

[Ru(dcbpyH$_2$)(dcbpyH)(L9)] (9). A degassed methanol (250 mL) solution charged with 75 mg (0.11 mmol) of **P9**, 53 mg (0.22 mmol) of $dcbpyH_2$ and 18 mg (0.44 mmol) of crushed NaOH was heated at reflux for 3 h. The solvent was then removed in vacuo, and the resultant solid was purified by column chromatography [SiO_2: ($MeOH/KNO_{3(aq,\ sat)}$/1% acetic acid 5:1:1)]. The isolated solid was reconstituted in H_2O and acidified with 0.2 M HNO_3 until the formation of a precipitate was observed. The solid was isolated, washed with H_2O and diethyl ether, and dried in vacuo to afford 65 mg (70%) of the product as a purple/red solid. ^{1}H NMR (CD_3OD with a drop of NaOD): δ 9.77 (s, 1H), 9.03 (s, 1H), 8.95 (d, ^4J = 1 Hz, 1H), 8.91 (d, ^4J = 1 Hz, 1H), 8.89 (d, ^4J = 1 Hz, 1H), 8.22 (m, 2H), 8.15 (dd, ^3J = 6 Hz, ^4J = 1 Hz, 1H), 7.92 (dd, ^3J = 6 Hz, ^4J = 1 Hz, 1H), 7.88−7.75 (m, ^3J = 6 Hz, ^4J = 1 Hz, 5H), 7.69 (dd, ^3J = 6 Hz, ^4J = 2 Hz, 1H), 7.66 (dd, ^3J = 6 Hz, ^4J = 2 Hz, 1H), 7.62 (dd, ^3J = 6 Hz, ^4J = 2 Hz, 1H), 7.60 (ddd, ^3J = 7 Hz, ^4J = 2 Hz, ^5J = 1 Hz, 1H), 7.55(d, ^3J = 4 Hz, 1H), 7.19 (dd, ^3J = 8 Hz, ^4J = 2 Hz, 1H), 7.03 (ddd, ^3J = 7 Hz, 6 Hz, ^4J = 1 Hz, 1H), 6.58 (d, ^3J = 8 Hz, 1H). HRMS (MALDI-TOF): m/z 854.0488 [M^+] (calcd for $C_{40}H_{26}N_5O_9SRu^+$: m/z 854.0500). Anal. Calcd. for $RuC_{40}H_{25}N_5O_9S + 3H_2O$: C, 52.98; H, 3.45; N, 7.72. Found: C, 53.05; H, 3.21; N, 7.70.

General Synthetic Procedure for 1a, 7a−9a. An aqueous (20 mL) suspension containing 0.112 mmol of **1** was titrated with 0.2 M tetrabutylammonium hydroxide (NBu_4OH) to reach pH 7. Solid impurities were removed by filtration, followed by the removal of solvent in vacuo. The resultant solid was reconstituted in MeOH and then drawn out of solution using a 1:1 mixture of diethyl ether/petroleum ether and purified by column chromatography [Sephadex LH-20: (H_2O)]. Solvent was removed from the dark purple fraction in vacuo leaving a solid that was dried overnight under reduced pressure to afford the product.

(Bu$_4$N)$_3$[Ru(dcbpy)(dcbpyH)(L1)]PF$_6$ (1a). Yield: 73 mg (40%) of the product as a dark purple solid. ^{1}H NMR (CD_3OD): δ 9.01 (s, 1H), 8.94 (s, 1H), 8.89 (s, 1H), 8.87 (s, 1H), 8.14 (dd, ^3J = 6 Hz, ^4J = 1 Hz, 1H), 8.06 (d, ^3J = 8 Hz, 1H), 7.91 (d, ^3J = 6 Hz, ^4J = 1 Hz, 1H), 7.88−7.84 (m, 3H), 7.79 (dd, ^3J = 6 Hz, ^4J = 1 Hz, 1H), 7.71 (ddd, ^3J = 9 Hz, 8 Hz, ^4J = 2 Hz, 1H), 7.67 (dd, ^3J = 6 Hz, ^4J = 2 Hz, 1H), 7.64 (dd, ^3J = 6 Hz, ^4J = 2 Hz, 1H), 7.60 (dd, ^3J = 6 Hz, ^4J = 2 Hz, 1H), 7.55 (ddd, ^3J = 6 Hz, ^4J = 2 Hz, ^5J = 1 Hz, 1H), 6.96 (ddd, ^3J = 7 Hz, 6 Hz, ^4J = 1 Hz, 1H), 6.90 (ddd, ^3J = 7 Hz, 7 Hz, ^4J = 1 Hz, 1H), 6.81 (ddd, ^3J = 7 Hz, 7 Hz, ^4J = 1 Hz, 1H), 6.40 (dd, ^3J = 7 Hz, ^4J = 1 Hz, 1H), 3.22 (m, 24H), 1.64 (m, 24H), 1.38 (sextet, ^3J = 7 Hz, 24H), 0.98 (t, ^3J = 7 Hz, 36H). ESI-MS: m/z = 744.2 [$(M - 3Bu_4N^+ + 4H^+)^+$] (calcd for $RuC_{35}H_{24}N_5O_8^+$: m/z = 744.1). Anal. Calcd. for $RuC_{83}H_{129}N_8O_8PF_6 + 4H_2O$: C, 59.16; H, 7.91; N, 6.81. Found: C, 59.42; H, 8.19; N, 6.65.

(Bu$_4$N)$_4$[Ru(dcbpy)$_2$(L3)]PF$_6$ (3a). A suspension containing 100 mg (0.107 mmol) of **1** in 20 mL of H_2O was titrated with 0.2 M NBu_4OH to reach pH 7 and then filtered. Removal of solvent in vacuo yielded an oily solid that was reconstituted in

MeOH and brought out of solution with a 1:1 mixture of diethyl ether/petroleum ether. The isolated solid was dried overnight under vacuum to afford 94 mg (46%) of a dark purple solid product. ^{1}H NMR (CD_3OD): δ 9.05 (s, 1H), 8.96 (s, 1H), 8.93 (s, 1H), 8.90 (s, 1H), 8.68 (d, ^4J = 2 Hz, 1H), 8.26 (d, ^3J = 8 Hz, 1H), 7.99 (d, ^3J = 6 Hz, 1H), 7.92−7.88 (m, 2H), 7.84−7.76 (m, 3H), 7.71 (dd, ^3J = 6 Hz, ^4J = 2 Hz, 1H), 7.68−7.60 (m, 3H), 7.56 (d, ^3J = 6 Hz, 1H), 7.10 (ddd, ^3J = 7 Hz, 6 Hz, ^4J = 1 Hz 1H), 6.75 (d, ^3J = 8 Hz, 1H), 3.23 (m, 32H), 1.65 (m, 32H), 1.40 (sextet, ^3J = 7 Hz, 32H), 1.00 (t, ^3J = 7 Hz, 48H). ESI-MS: m/z = 789.1 [(M − 3Bu$_4$N$^+$ + 4H$^+$)$^+$] (calcd for $RuC_{35}H_{23}N_6O_{10}^+$: m/z = 789.1). Anal. Calcd. for $RuC_{99}H_{171}N_{10}O_{14}PF_6 + 4H_2O$: C, 60.31; H, 8.74; N, 7.10. Found: C, 60.40; H, 8.47; N, 7.39.

(Bu$_4$N)$_3$[Ru(dcbpy)(dcbpyH)(L6)]PF$_6$ (6a). A suspension containing 100 mg (0.108 mmol) of **6** in 20 mL of H_2O was titrated using 0.2 M NBu$_4$OH to reach pH 7. A reaction workup identical to that of **3a** affords 80 mg (45%) of the product as a dark purple solid. ^{1}H NMR (CD_3OD): δ 9.03 (s, 1H), 8.96 (s, 1H), 8.92 (s, 1H), 8.91 (s, 1H), 8.31 (d, ^3J = 8 Hz, 1H), 8.09 (d, ^3J = 6 Hz, 1H), 7.89−7.85 (m, 2H), 7.80−7.62 (m, 7H), 7.00 (t, ^3J = 6 Hz, 1H), 6.38 (ddd, ^3J = 13 Hz, 9 Hz, ^4J = 2 Hz, 1H), 5.90 (dd, ^3J = 6 Hz, ^4J = 1 Hz, 1H), 3.23 (m, 24H), 1.64 (m, 24H), 1.38 (sextet, ^3J = 7 Hz, 24H), 0.98 (t, ^3J = 7 Hz, 36H). ESI-MS: m/z = 780.1 [(M − 3Bu$_4$N$^+$ + 4H$^+$)$^+$] (calcd for $RuC_{35}H_{22}F_2N_5O_8^+$: m/z = 780.1). Anal. Calcd. for $RuC_{83}H_{127}F_8N_8O_8P$: C, 60.46; H, 7.76; N, 6.80. Found: C, 60.78; H, 8.26; N, 6.75.

(Bu$_4$N)$_3$[Ru(dcbpy)$_2$(L7)] (7a). Yield: 48 mg (62%) of the product as a dark purple solid. ^{1}H NMR (CD_3OD): δ 9.03 (s, 1H), 8.95 (s, 1H), 8.91 (s, 1H), 8.89 (s, 1H), 8.22 (m, 2H), 8.13 (d, ^4J = 2 Hz, 1H), 7.94 (d, ^3J = 6 Hz, 1H), 7.87 (m, 2H), 7.83 (d, ^3J = 6 Hz, 1H), 7.74 (ddd, ^3J = 8 Hz, 7 Hz, ^4J = 2 Hz, 1H), 7.68 (dd, ^3J = 6 Hz, ^4J = 2 Hz, 1H), 7.66−7.61 (m, 4H), 7.57 (d, ^3J = 6 Hz, 1H), 7.38 (t, ^3J = 7 Hz, 2H), 7.24 (t, ^3J = 7 Hz, 1H), 7.12 (dd, ^3J = 8 Hz, ^4J = 2 Hz, 1H), 6.99 (ddd, ^3J = 7 Hz, 6 Hz, ^4J = 1 Hz, 1H), 6.53 (d, ^3J = 8 Hz, 1H), 3.20 (m, 24H), 1.62 (m, 24H), 1.37 (sextet, ^3J = 7 Hz, 24H), 0.97 (t, ^3J = 7 Hz, 36H). ^{13}C NMR (CD_3OD): 193.3, 171.3, 171.1, 171.0, 168.8, 159.4, 158.7, 158.3, 157.0, 155.4, 151.3, 151.1, 151.0, 150.2, 147.9, 147.4, 146.4, 145.3, 145.0, 143.5, 137.3, 136.9, 135.6, 129.9, 128.5, 127.8, 127.6, 127.4, 127.0, 126.6, 124.0, 123.9, 123.8, 123.7, 123.6, 123.5, 120.4, 59.7, 24.9, 20.8, 14.1. ESI-MS: m/z = 820.1 [(M − 3Bu$_4$N$^+$ + 4H$^+$)$^+$] (calcd for $RuC_{41}H_{28}N_5O_8^+$: m/z = 820.1). Anal. Calcd. for $RuC_{89}H_{148}N_8O_{16} + 8H_2O$: C, 63.36; H, 8.84; N, 6.64. Found: C, 63.57; H, 8.64; N, 6.59.

(Bu$_4$N)$_3$[Ru(dcbpy)$_2$(L8)] (8a). Yield: 36 mg (84%) of the product as a dark purple solid. ^{1}H NMR (CD_3OD): δ 9.05 (s, 1H), 8.96 (d, ^4J = 1 Hz, 1H), 8.92 (d, ^4J = 1 Hz, 1H), 8.89 (d, ^4J = 1 Hz, 1H), 8.49 (d, ^3J = 6 Hz, 2H), 8.28 (m, 2H), 8.17 (dd, ^3J = 6 Hz, ^4J = 1 Hz, 1H), 7.94 (dd, ^3J = 6 Hz, ^4J = 1 Hz, 1H), 7.89−7.82 (m, 3H), 7.80−7.75 (m, 3H), 7.70 (dd, ^3J = 6 Hz, ^4J = 2 Hz, 1H), 7.66 (dd, ^3J = 6 Hz, ^4J = 2 Hz, 1H), 7.61 (m, 2H), 7.25 (dd, ^3J = 8 Hz, ^4J = 2 Hz, 1H), 7.03 (ddd, ^3J = 7 Hz, 6 Hz, ^4J = 1 Hz, 1H), 6.63 (d, ^3J = 8 Hz, 1H), 3.22 (m, 24H), 1.63 (m, 24H), 1.38 (sextet, ^3J = 7 Hz, 24H), 0.98 (t, ^3J = 7 Hz, 36H). ^{13}C NMR (CD_3OD): 199.1, 171.1, 170.9, 170.8, 168.4, 159.3, 158.7, 158.3, 156.9, 155.3, 151.8, 151.4, 151.1, 151.0, 150.4, 150.2, 148.1, 146.6, 145.5, 137.5, 131.4, 127.8, 127.6, 127.1, 126.7, 124.1, 124.0, 123.8, 123.7, 123.0, 122.4, 120.7, 59.6, 24.9, 20.8, 14.1. ESI-MS: m/z = 821.2 [(M − 3Bu$_4$N$^+$ + 4H$^+$)$^+$] (calcd for $RuC_{40}H_{27}N_6O_8^+$: m/z = 821.1). Anal. Calcd. for $RuC_{88}H_{147}N_9O_{16} + 8H_2O$: C, 62.61; H, 8.78; N, 7.47. Found: C, 62.43; H, 8.72; N, 7.26.

(Bu$_4$N)$_3$[Ru(dcbpy)$_2$(L9)] (9a). Yield: 45 mg (59%) of the product as a dark purple solid. ^{1}H NMR (CD_3OD): δ 9.80 (s, 1H), 9.04 (s, 1H), 8.96 (d, ^4J = 1 Hz, 1H), 8.92 (d, ^4J = 1 Hz, 1H), 8.89 (d, ^4J = 1 Hz, 1H), 8.24 (m, 2H), 8.15 (dd, ^3J = 6 Hz, ^4J = 1 Hz, 1H), 7.93 (dd, ^3J = 6 Hz, ^4J = 1 Hz, 1H), 7.89−7.76 (m, ^3J = 6 Hz, ^4J = 1 Hz, 5H), 7.70 (dd, ^3J = 6 Hz, ^4J = 2 Hz, 1H), 7.66 (dd, ^3J = 6 Hz, ^4J = 2 Hz, 1H), 7.63 (dd, ^3J = 6 Hz, ^4J = 2 Hz, 1H), 7.61 (ddd, ^3J = 7 Hz, ^4J = 2 Hz, ^5J = 1 Hz, 1H), 7.57(d, ^3J = 4 Hz, 1H), 7.19 (dd, ^3J = 8 Hz, ^4J = 2 Hz, 1H), 7.04 (ddd, ^3J = 7 Hz, 6 Hz, ^4J = 1 Hz, 1H), 6.59 (d, ^3J = 8 Hz, 1H), 3.21 (m, 24H), 1.63 (m, 24H), 1.38 (sextet, ^3J = 7 Hz, 24H), 0.98 (t, ^3J = 7 Hz, 36H). ^{13}C NMR (CD_3OD): 200.7, 184.8, 168.0, 159.3, 158.7, 158.3, 156.8, 155.3, 151.5, 151.3, 150.3, 148.0, 141.7, 140.6, 137.6, 137.3, 127.9, 127.5, 127.2, 127.0, 126.8, 124.3, 124.2, 124.1, 124.0, 123.8, 123.7, 122.1, 120.7, 59.6, 24.9, 20.9, 14.1. HRMS (ESI): m/z = 854.04918 [(M − 3Bu$_4$N$^+$ + 4H$^+$)$^+$] (calcd for $RuC_{40}H_{26}N_5O_9S^+$: m/z = 854.04947). Anal. Calcd. for $RuC_{88}H_{146}N_8O_{17}S + 8H_2O$: C, 61.40; H, 8.55; N, 6.51. Found: C, 61.07; H, 7.89; N, 6.44.

Physical Methods. Routine ^{1}H and ^{13}C NMR spectra were recorded at 400 and 100 MHz, respectively, on a Bruker AV 400 instrument at ambient temperature unless otherwise stated. Elemental analysis (EA), electrospray ionization mass spectrometry (ESI-MS), matrix-assisted laser desorption/ionization mass spectrometry (MALDI-TOF), and electron impact (EI) mass spectrometry data were collected at the University of Calgary. Electrochemical measurements were performed under anaerobic conditions with a Princeton Applied Research VersaStat 3 potentiostat using dry solvents, Pt working and counter electrodes, a Ag pseudoreference electrode, and 0.1 M NBu$_4$BF$_4$ supporting electrolyte. Electronic spectroscopic data were collected on MeOH solutions using a Cary 5000 UV−vis spectrophotometer (Varian). Steady-state emission spectra were obtained at room temperature using an Edinburgh Instruments FLS920 Spectrometer equipped with a Xe900 450W steady state xenon arc lamp, TMS300-X excitation monochromator, TMS300-M emission monochromator, Hamamatsu R2658P PMT detector and corrected for detector response. Lifetime measurements were obtained at room temperature using an Edinburgh Instruments FLS920 Spectrometer equipped with Fianium SC400 Super Continuum White Light Source, Hamamatsu R3809U-50 Multi Channel Plate detector and data were analyzed with Edinbrugh Instruments F900 software. Curve fitting of the data was performed using a nonlinear least-squares procedure in the F900 software.

DFT Calculations. Density functional theory (DFT) calculations were carried out using B3LYP[42−45] (Becke's three-parameter exchange functional (B3) and the Lee−Yang−Parr correlation functional (LYP)) and the LanL2DZ basis set.[46−49] All geometries were fully optimized in the ground states (closed-shell singlet S_0). Time-dependent density functional theory (TD-DFT) calculations were performed with IEFPCM solvation model (MeCN)[50] using a spin-restricted formalism to examine low-energy excitations at the ground-state geometry (output files are provided as Supporting Information). All calculations were carried out with the Gaussian 03W software package.[51]

Results

Synthesis and Structural Characterization. Cyclometalated Ru(II) complexes of the form [Ru(dcbpyH$_2$)$_2$-($C^\wedge N$)]$^+$ can be accessed using one of these two general routes: (i) initial coordination of the dcbpyH$_2$ ligands to

(42) Becke, A. D. *Phys. Rev. A: Gen. Phys.* **1988**, *38*, 3098–3100.
(43) Becke, A. D. *J. Chem. Phys.* **1993**, *98*, 5648–5652.
(44) Lee, C.; Yang, W.; Parr, R. G. *Phys. Rev. B: Condens. Matter* **1988**, *37*, 785–789.
(45) Miehlich, B.; Savin, A.; Stoll, H.; Preuss, H. *Chem. Phys. Lett.* **1989**, *157*, 200–206.
(46) Dunning, T. H., Jr.; Hay, P. J. *Mod. Theor. Chem.* **1977**, *3*, 1–27.
(47) Hay, P. J.; Wadt, W. R. *J. Chem. Phys.* **1985**, *82*, 270–283.
(48) Hay, P. J.; Wadt, W. R. *J. Chem. Phys.* **1985**, *82*, 299–310.
(49) Wadt, W. R.; Hay, P. J. *J. Chem. Phys.* **1985**, *82*, 284–298.
(50) The solvent model was not used for **7** and **8**.
(51) Frisch, M. J.; et al. *Gaussian 03*, Revision c02; Gaussian Inc.: Wallingford, CT, 2004.

the Ru center followed by cyclometalation; or (ii) initial activation of the C−H bond to furnish a cyclometalated Ru site with subsequent coordination of the dcbpyH_2 ligands. While the first method is typically employed to isolate compounds of type [Ru($N^{\wedge}N$)$_2$($C^{\wedge}N$)]$^+$,[16−19,21,30] the latter approach has been shown to converge on a number of heteroleptic Ru(II)[26,27,34,52−54] and Ir[55−58] complexes. The syntheses described in this study follow this latter approach because it generates high yields under mild reaction conditions and eliminates the occurrence of undesirable isomerization products when Ru(dcbpyH_2)$_2$$Cl_2$ is utilized as a synthon.

The installation of various substituents (e.g., −NO_2, −F, −4-phenyl, −4-pyridine, −thiophene-2-carbaldehyde) on the cyclometalating 2-phenylpyridine ligand was achieved in moderate to high yields using standard Negishi or Suzuki cross-coupling reaction conditions. Noting that [(η^6-C_6H_6)RuCl_2]$_2$ has been documented to be a useful precursor in cyclometalation reactions,[27] we carried out the requisite C−H activation of the cyclometalating ligands using [(η^6-*p*-cymene)RuCl_2]$_2$.[59,60] The reaction workup can be carried out in ambient conditions, which contrasts with the anaerobic conditions required for reactions involving [(η^6-C_6H_6)RuCl_2]$_2$. For all of the ligands used in this study, the reaction generated a solution containing two products, [(η^2-*p*-cymene)Ru(MeCN)$_2$(**L#**)]PF_6 and [Ru(MeCN)$_4$(**L#**)]PF_6. Monitoring the reaction by ^{1}H NMR spectroscopy indicates that [(η^2-*p*-cymene)Ru(MeCN)$_2$(**L#**)]PF_6 is formed initially, and is progressively converted to [Ru(MeCN)$_4$(**L#**)]PF_6 over the course of the reaction.[27] Both of these species afford the respective target metal complex (i.e., **1**−**9**) when combined with 2 equiv of dcbpyH_2; however, greater emphasis was placed on ensuring that [(η^6-*p*-cymene)-RuCl_2]$_2$ was completely consumed rather than separating the two intermediate species. We therefore do not offer the synthesis and characterization details for most of these precursors; however, the data for **P1** and **P5** is included as a representative sample. Complexes **1**−**9** were obtained in reasonably high yields after refluxing the corresponding precursor mixtures **P1**−**P9** with NaOH and dcbpyH_2 in degassed (aqueous) methanol. The fully protonated forms of complexes **1**−**6** were isolated by the dropwise addition of HPF_6 to the reaction mixture until the products precipitated out of solution; acidification of **7**, **8**, and **9** with HNO_3 produced zwitterionic compounds rather than the respective NO_3^- salts. Compound **8** exists as the pyridinium salt as a consequence of the acidification process.

The structural identities of the compounds were verified by a combination of elemental analysis, MALDI-TOF, ESI-MS, ^{1}H NMR, and/or ^{13}C NMR spectroscopy. Representative ^{1}H NMR spectra are provided in the Supporting Information. The signature upfield doublet observed at 6.39 ppm in the ^{1}H NMR spectrum of **1**, emanating from the proton adjacent to the Ru−C bond, did not always serve as a useful spectroscopic handle because it is, in certain cases, drawn downfield to overlap with other aromatic signals. Because of inherent solubility issues, compounds **1**, **3**, and **6**−**9** were deprotonated by adjusting the pH to 7 using NBu_4OH;[61] these hygroscopic compounds are all soluble in polar organic solvents. ^{1}H NMR spectroscopy and elemental analysis were used to establish that **3a** is fully deprotonated, and that **1a**, **6a**, **7a**, **8a**, and **9a** all contain three NBu_4^+ counterions. This disparity is ascribed to the stronger electron-withdrawing character of the −NO_2 group lowering the pK_a of the acid modalities. Diastereomers of complexes **7a**−**9a** were not observed because poor solubility precluded the collection of NMR data in solvents (e.g., hexanes, chloroform) that restrict proton exchange. Thermogravimetric and elemental analysis data collectively confirm the hygroscopic nature of the deprotonated complexes (no less than 5 H_2O molecules are present in solid samples of **7a**−**9a**).[61]

Electrochemical Properties. The electrochemical behavior for **1**−**6** in DMF was determined by cyclic voltammetry. Solubility issues precluded the collection of satisfactory voltammograms for **1** and **7**−**9**; thus, deprotonated forms of select compounds (i.e., **1a**, **3a**, **6a**−**9a**) were prepared to facilitate a comprehensive comparison of the series. Relevant redox couples are collected in Table 1.

The voltammograms for all of the complexes reveal a reversible one-electron metal-based oxidation process and a series of reduction processes. Compound **1a** exhibits a single reversible wave ascribed to the one-electron reduction of a dcbpy ligand. For the −NO_2 series **2**−**5**, the cathodic sweep leads to the reduction of the −NO_2 group of the $C^{\wedge}N$ ligand. Compound **5**, which contains two −NO_2 groups, exhibits a reduction potential about 0.23 V lower than those containing a single −NO_2 group. The reduction of **6**, which contains two strong electron-withdrawing −F groups, involves the dcbpyH_2 groups, thereby demonstrating that the −NO_2 group exhibits superior electron-withdrawing character. Inspection of **2**−**4** indicates the complexes are most easily oxidized when the −NO_2 groups are *meta* to the organometallic bond: the additional −NO_2 group for **5** leads to an oxidation potential that is anodically shifted by an additional ∼100 mV relative to **2**−**4**. The placement of the aromatic substituents *para* to the organometallic bond reveals progressively higher oxidation potentials for **7a**−**9a**, respectively, thus reflecting the relative electron-withdrawing character of the substituents. Compounds **7a**−**9a**

(52) Saavedra-Diaz, O.; Ceron-Camacho, R.; Hernandez, S.; Ryabov, A. D.; Le Lagadec, R. *Eur. J. Inorg. Chem.* **2008**, 4866–4869.
(53) Ryabov, A. D.; Estevez, H.; Alexandrova, L.; Pfeffer, M.; Le Lagadec, R. *Inorg. Chim. Acta* **2006**, *359*, 883–887.
(54) Ryabov, A. D.; Le Lagadec, R.; Estevez, H.; Toscano, R. A.; Hernandez, S.; Alexandrova, L.; Kurova, V. S.; Fischer, A.; Sirlin, C.; Pfeffer, M. *Inorg. Chem.* **2005**, *44*, 1626–1634.
(55) Duan, L. L.; Fischer, A.; Xu, Y. H.; Sun, L. C. *J. Am. Chem. Soc.* **2009**, *131*, 10397–10399.
(56) Lowry, M. S.; Bernhard, S. *Chem.—Eur. J.* **2006**, *12*, 7970–7977.
(57) Duan, H.-S.; Chou, P.-T.; Hsu, C.-C.; Hung, J.-Y.; Chi, Y. *Inorg. Chem.* **2009**, *48*, 6501–6508.
(58) Lee, T.-C.; Hung, J.-Y.; Chi, Y.; Cheng, Y.-M.; Lee, G.-H.; Chou, P.-T.; Chen, C.-C.; Chang, C.-H.; Wu, C.-C. *Adv. Funct. Mater.* **2009**, *19*, 2639–2647.
(59) Kuznetsov, V. F.; Abdur-Rashid, K.; Lough, A. J.; Gusev, D. G. *J. Am. Chem. Soc.* **2006**, *128*, 14388–14396.
(60) Steenwinkel, P.; James, S. L.; Gossage, R. A.; Grove, D. M.; Kooijman, H.; Smeets, W. J. J.; Spek, A. L.; van Koten, G. *Organometallics* **1998**, *17*, 4680–4693.
(61) Nazeeruddin, M. K.; Zakeeruddin, S. M.; Humphry-Baker, R.; Jirousek, M.; Liska, P.; Vlachopoulos, N.; Shklover, V.; Fischer, C.-H.; Grätzel, M. *Inorg. Chem.* **1999**, *38*, 6298–6305.

Table 1. Electrochemical and Electronic Spectroscopy Data for Cyclometalated Ru(II) Compounds

compound	UV−vis data[a]				$E_{1/2}$ (V vs NHE)[b]		
	λ_{max1} (nm)	λ_{max2} (nm)	λ_{max3} (nm)	λ_{em} (nm)[a]	E_{ox1}	E_{red1}	$E(S^+/S^*)$(V vs NHE)[c]
$[Ru(dcbpyH_2)_2(\mathbf{L1})]PF_6$ (**1**)	575	503	413	827	–[f]	–	–
$[Ru(dcbpyH_2)_2(\mathbf{L2})]PF_6$ (**2**)	554 (0.9)	491 (0.8)	405 (1.1)	–	+1.09	−0.96[g]	–
$[Ru(dcbpyH_2)_2(\mathbf{L3})]PF_6$ (**3**)	545 (1.9)	494 (1.8)	405 (2.2)	794	+1.12	−0.95[g]	−0.67
$[Ru(dcbpyH_2)_2(\mathbf{L4})]PF_6$ (**4**)	557 (1.9)	–[e]	401 (1.7)	–	+1.08	−0.94[g]	–
$[Ru(dcbpyH_2)_2(\mathbf{L5})]PF_6$ (**5**)	532 (1.2)	–[e]	379 (1.2)	–	+1.21	−0.72[g]	–
$[Ru(dcbpyH_2)_2(\mathbf{L6})]PF_6$ (**6**)[30]	557 (1.6)	489 (1.1)	404 (1.7)	803	+1.06	−1.01[g]	−0.70
$(Bu_4N)_3[Ru(dcbpy)(dcbpyH)(\mathbf{L1})]PF_6$ (**1a**)	563 (2.0)	496 (1.6)	409 (2.3)	810	+0.64	−1.47	−1.10
$(Bu_4N)_4[Ru(dcbpy)_2(\mathbf{L3})]PF_6$ (**3a**)	530 (2.0)	–[e]	393 (1.9)	781	+0.80	−1.12	−0.99
$(Bu_4N)_3[Ru(dcbpy)(dcbpyH)(\mathbf{L6})]PF_6$ (**6a**)	545 (2.0)	485 (1.5)	401 (2.3)	770	+0.76	−1.46	−1.04
$(Bu_4N)_3[Ru(dcbpy)_2(\mathbf{L7})]$ (**7a**)	563 (1.6)[d]	497 (1.3)	408 (1.8)	802	+0.61	−1.50	−1.12
$(Bu_4N)_3[Ru(dcbpy)_2(\mathbf{L8})]$ (**8a**)	556 (1.6)[d]	494 (1.4)	382 (2.4)	794	+0.65	−1.49	−1.12
$(Bu_4N)_3[Ru(dcbpy)_2(\mathbf{L9})]$ (**9a**)	550 (1.7)[d]	492 (2.2)	412 (2.8)	788	+0.68	−1.45	−1.08

[a] Recorded in MeOH; ε values indicated in parentheses with units of $\times 10^4$ M^{-1} cm^{-1}. [b] Data collected using 0.1 M NBu_4BF_4 DMF solutions at 200 mV/s and referenced to a $[Fc]/[Fc]^+$ internal standard followed by conversion to NHE ($[Fc]/[Fc]^+$ vs NHE = 0.69 V).[62] [c] Calculated using $E(S^+/S^*) = E(S^+/S) - E^{(0-0)}$, where $E^{(0-0)}$ is obtained from the higher energy side of corrected emission band where the intensity is ca. 10% of the maximum.[30] [d] λ_{max1} = 577, 564, and 564 nm for **7**−**9**, respectively. [e] Observed as shoulder of λ_{max1}. [f] Could not be accurately measured because of poor solubility. [g] (Quasi-)irreversible; $E_{p,c}$ reported.

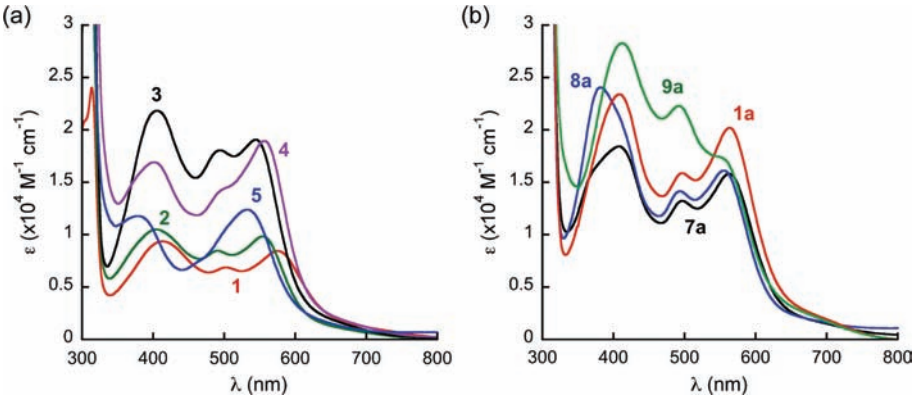

Figure 3. Electronic absorption spectra for (a) the $-NO_2$ series **2**−**5**, and (b) **7a**−**9a**, which contain aromatic substituents. The spectra for benchmark complexes **1** and **1a** are included in the respective plots.[63]

exhibit a single reversible reduction wave at comparable potentials consistent with the reduction of the dcbpy ligands.

Electronic and Fluorescence Spectroscopy. The spectral profile for each compound studied contains three broad absorption bands in the visible region centered at roughly 540, 490, and 400 nm (maxima are denoted as λ_{max1}, λ_{max2}, and λ_{max3}, respectively, in Table 1) along with intense intraligand ($\pi-\pi^*$) transitions below 350 nm. Representative UV−vis absorption spectra are depicted in Figure 3. The two low-energy bands are superimposed in the cases of **3a**, **4**, and **5**. The bands in the visible region for all of the compounds are ascribed to a collection of mixed-metal/ligand to ligand charge-transfer transitions arising from a HOMO involving both the metal and the anionic portion of the *C^N* ligand. Electrochemical measurements indicate that significant electron density is situated on the metal; thus, these transitions are, for the sake of brevity, defined herein as metal-to-ligand charge-transfer (MLCT).[34]

The maxima for the lowest-energy MLCT bands are found over the 532−575 nm range for the series **1**−**5**. There is a direct correlation between the number of $-NO_2$ groups present and λ_{max} values, namely, the λ_{max1} values are found at the lowest energy for **1** and the highest energy for **5**, while the monosubstituted nitro derivatives **2**−**4** exhibit intermediate λ_{max1} values. The λ_{max3} values adhere to this same trend. Data for **3** reveals a lower λ_{max1} value relative to the compounds where the $-NO_2$ group is situated *meta* to the organometallic bond. This trend is consistent with enhanced π-electron conjugation for **3** leading to a lower-energy HOMO level relative to the cross-conjugated systems **2** and **4**. The molar extinction coefficients (ε) are found to range from 1×10^4−2×10^4 $M^{-1}cm^{-1}$ over the series. The ε value of 0.9×10^4 $M^{-1}cm^{-1}$ for the signal at λ_{max1} for **2** is less than half that of **3** or **4** ($\varepsilon = 1.9 \times 10^{-4}$ M^{-1} cm^{-1}). The diminished intensity of this band is presumably a consequence of the loss of conjugation in **2** arising from steric interactions between the H atom on the adjacent pyridyl ring and the $-NO_2$ group. Compound **4** is not subject to this steric encumbrance; thus, the $-NO_2$ group can reside in the plane of the aromatic rings of the *C^N* ligand.

The UV−vis data for the deprotonated analogues **7a**−**9a** reveal that the lowest-energy transitions occur at 563, 556, and 550 nm, respectively. The relative intensities of the three maxima in the visible region indicate that the ε value for λ_{max1} and λ_{max3} increases for **7a**−**9a**, respectively. A hypsochromic shift of the λ_{max1} and λ_{max2} values is observed with progressively stronger electron-withdrawing groups (EWGs). This trend reflects a diminished level of π-backbonding to $dcbpyH_2$ as the

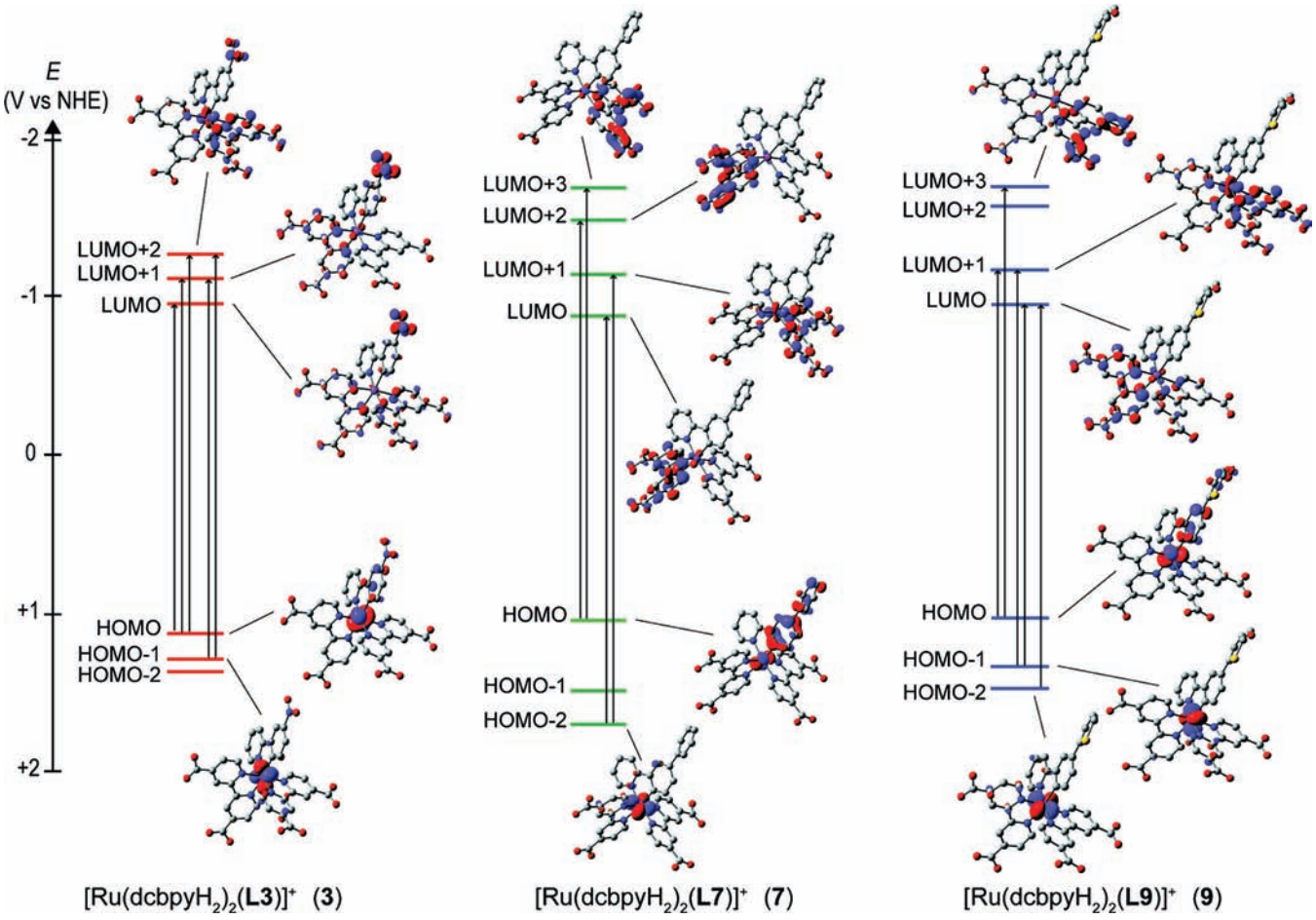

Figure 4. Energy level diagrams depicting the dominant transitions that comprise the lowest-energy absorption band λ_{max1} for **3**, **7**, and **9**. (Transitions that are predicted to contribute less than 10% to the absorbance band are omitted. Color scheme: Ru = magenta; O = red; N = blue; C = gray; H atoms not shown.).

aromatic moiety of the $C^{\wedge}N$ ligand becomes more electron withdrawing. The increasing ε for λ_{max3} is the result of an increasing number of transitions to the $C^{\wedge}N$ ligand and enhanced conjugation between the adjacent aromatic rings (vide infra). The λ_{max3} band is more intense with increasing electron-withdrawing character of the aromatic substituent. Consequently, **9a** exhibits the greatest absorption envelope in the visible region of any of the compounds studied in this work.

Fluorescence data indicates that emission is quenched in cases where cross-conjugation is present in the $-NO_2$ series, that is, where $-NO_2$ groups are installed at either one or both $-$*meta* positions relative to the Ru−C bond. Complexes containing −F groups or substituents installed *para* to the Ru−C bond are all weakly emissive when excited at wavelengths corresponding to λ_{max1}, and display lifetimes over the 2−40 ns range.

TD-DFT Calculations. TD-DFT calculations were carried out on geometry-optimized structures of the metal complexes using a B3LYP/LanL2DZ level of theory to qualitatively assess the frontier molecular orbitals. The low level of symmetry within these systems leads to a relatively complicated orbital structure and an increase in the number of allowed electronic transitions (hence the broader absorption profiles). The predicted low-energy transitions are blue-shifted approximately 5−9 nm compared to the experimental values listed in Table 1. All predicted UV−vis spectra and transitions at $\lambda > 400$ nm are available in the Supporting Information.

An evaluation of the electronic transitions by TD-DFT indicates that the low-energy excitation bands arise from a set of mixed-metal/ligand-to-ligand charge-transfer transitions from the predominantly metal-based d_{xz}, d_{yz}, d_{xy} orbitals to a set of π^* orbitals with exclusively $dcbpyH_2$ character. Although numerous transitions comprise each of the three absorption bands in the visible region for all of the complexes, a reduction of the TD-DFT results reveals some overarching trends. The lowest-energy band λ_{max1}, for instance, involves excited states localized primarily to the π^* system of the $dcbpyH_2$ ligand *cis* to the anionic fragment of the $C^{\wedge}N$ ligand. Absorption band λ_{max2} arises from the population of the π^* orbitals of the $dcbpyH_2$ ligand *trans* to the phenyl ring bound to the Ru site, while the higher energy band at about 400 nm (λ_{max3}) involves a more significant participation of the π^* orbitals belonging to the $C^{\wedge}N$ ligand. Anomalous behavior is observed for **3** because the low-lying empty orbitals contain more $C^{\wedge}N$ character.

The dominant allowed transitions that comprise the lowest-energy absorption band, λ_{max1}, are depicted schematically for **3**, **7**, and **9** in Figure 4. The d_{yz}, d_{xy} and d_{xz} orbitals comprise the three highest occupied molecular orbitals for compounds **1**−**7** and **9**; however, they are not degenerate because of the C_1 symmetry. For complex **8**,

the HOMO−1 orbital is situated solely on the pendant pyridine moiety, and the d_{xz} and d_{xy} orbitals are found at the HOMO−2 and HOMO−3 levels. In general, the HOMO is a linear combination of the metal d_{yz} orbital and the anionic phenyl ring of the *C^N* ligand with empty low-lying orbitals extended over the π^* system of the $dcbpyH_2$ ligands. For **2**, **4**, and **5**, however, the lowest energy excited states are localized to the phenyl ring and the $-NO_2$ group(s) of the *C^N* ligand. For **3**, where the $-NO_2$ group is *para* to the organometallic bond, the lowest unoccupied levels involve both the $dcbpyH_2$ ligands and the nitrophenyl scaffold; the HOMO is a mixture of the d_{yz} orbital and nitrophenyl moiety.

The addition of aromatic substituents to the *C^N* ligand results in an expansion of the HOMO to include the phenyl, 4-pyridine, and thiophene-2-carbaldehyde moieties in **7**−**9**, respectively. There is an enhancement of orbital character over the aromatic scaffold of **9** compared to **7** and **8** because of the relatively small dihedral angle between the phenyl group of the *C^N* ligand and the thiophene substituent. Electronic transitions comprising the low energy excitation MLCT band for **7**−**9** occur from the metal d_{xz}, d_{yz}, d_{xy} orbitals to LUMOs localized to the $dcbpyH_2$ ligands; the *C^N* π^* orbitals are found to be 1.4, 1.4, and 0.7 eV higher in energy than the LUMO in **7**−**9**, respectively.

Discussion. Compounds **2**−**9** were designed to gain insight into how the nature, position, and number of substituents affect the electrochemical and optical properties of cyclometalated chromophores related to **1**. The central aim of this study is to exploit the mixed-metal/ligand character of the HOMO for **1** by placing conjugated substituents on the anionic fragment of the bidentate *C^N* ligand while holding the balance of the structure at parity. This investigation is part of our larger effort to develop chromophores for sensitization applications; thus, the remaining coordination sphere for each of the compounds is occupied by two polypyridyl $dcbpyH_2$ ligands, a common linker for binding metal complexes to semiconducting surfaces in energy conversion schemes such as the DSSC.

The series of compounds selected for this study include complexes where the *C^N* ligand of **1** contains $-NO_2$ groups positioned about the phenyl ring (i.e., **2**−**5**). These nitro-substituted derivatives were evaluated to verify that optimal electronic coupling is achieved by placing the $-NO_2$ group *para* to the organometallic bond. We set out to demonstrate that by extending the HOMO and optical cross-section of the molecule large ε values could be produced as a result of the increased charge separation distance in the excited state;[64−66] thus, we furnished the *C^N* ligand of **1** with aromatic substituents to form **7**−**9**. For the purposes of generating dyes for the DSSC where I^-/I_3^- is used as the electrolyte, the HOMO energy level must be appropriately positioned to accommodate a sufficiently large driving force for dye regeneration.[1,30,67,68] For this reason, electron-withdrawing substituents on the *C^N* ligand are desirable to avoid raising the energy of the HOMO level above that of the redox couple of the electrolyte; that is, $E_{ox} > \sim 0.5$ V versus NHE. This line of reasoning prompted us to study how the oxidation potential of **7** is affected when the phenyl substituent is replaced with the −4-pyridyl group of **8**. Compound **9** was prepared in this same vein by utilizing an aldehyde to withdraw electron density from the metal; this compound also provides a platform for examining how the torsional strain between adjacent aromatic rings affects the optical properties.

The *C^N* ligands **HL2**−**HL9** are all readily accessible through carbon−carbon cross-coupling procedures. The general synthetic protocol for isolating the target complexes **1**−**9** was achieved using an initial cyclometalation step to form a cyclometalated intermediate(s) followed by coordination of the polypyridyl $dcbpyH_2$ ligands. This strategy offers numerous advantages to the established method of synthesizing derivatives of **1**. For instance, the more common approach of binding the *C^N* ligand to *cis*-$Ru(dcbpyH_2)_2Cl_2$ requires that the metal precursor be kept in the dark to avoid isomerization to the *trans* form. This route also generates homoleptic byproducts that ultimately lower the yields of reactions involving *cis*-$Ru(dcbpyH_2)_2Cl_2$. Not only are said obstacles overcome with the synthetic route described herein, but our protocol also provides a more efficient pathway for isolating Ru dyes containing a combination of bidentate polypyridyl and *C^N* ligands.

The electrochemical properties of the entire series exhibit an exquisite sensitivity to substituents on the *C^N* ligand. The reversibility of the oxidation wave indicates that the metal is the primary redox-active component;[34] however, the E_{ox} values are particularly responsive to substituents on the phenyl ring arising from the direct interaction with the HOMO that is extended over the ligand. For instance, the presence of one $-NO_2$ group increases the E_{ox} value by 0.16 V relative to **1a**. The highest E_{ox} value is observed for **3** among the complexes containing a single $-NO_2$ group because the substituent is situated *para* to the organometallic bond. The (quasi-) irreversibility of the first reduction waves for **2**−**5** is consistent with reduction of the $-NO_2$ groups; however, the first reduction process for **3** may also involve the $dcbpyH_2$ ligands. This possibility is supported by a quasi-reversible reduction wave, TD-DFT calculations and the observation of a weak emission signal for **3a**. Our data also shows that a single $-NO_2$ group increases the E_{ox} value more than the presence of two −F substituents.

Despite the observation that the LUMO is localized primarily to the $-NO_2$ group(s), these compounds provide some promising insight in the context of chromophore design for light-harvesting applications; namely, the extension of the π-system of the *C^N* ligand clearly leads to a significant increase in ε values. This feature is

(62) Pavlishchuk, V. V.; Addison, A. W. *Inorg. Chim. Acta* **2000**, *298*, 97–102.
(63) Note that the intensity of **1** may be diminished because of poor solubility.
(64) Brunschwig, B. S.; Creutz, C.; Sutin, N. *Coord. Chem. Rev.* **1998**, *177*, 61–79.
(65) Karki, L.; Lu, H. P.; Hupp, J. T. *J. Phys. Chem.* **1996**, *100*, 15637–15639.
(66) Groenen, E. J. J.; Van Velzen, P. N. T. *Mol. Phys.* **1977**, *33*, 933–942.
(67) Hagberg, D. P.; Marinado, T.; Karlsson, K. M.; Nonomura, K.; Qin, P.; Boschloo, G.; Brinck, T.; Hagfeldt, A.; Sun, L. *J. Org. Chem.* **2007**, *72*, 9550–9556.
(68) Koops, S. E.; O'Regan, B. C.; Barnes, P. R. F.; Durrant, J. R. *J. Am. Chem. Soc.* **2009**, *131*, 4808–4818.

reflected by broad absorption bands with ε values that can be 2-fold greater than that of **1**. Compound **3**, for instance, exhibits the most intense profile of the entire series. This observation emphasizes the importance of delocalizing the ground-state orbital character as a means of increasing the optical cross-section of the dye. On this basis, conjugated substituents were installed *para* to the Ru−C bond in pursuit of complexes with significantly higher intensity absorption bands relative to **1**. The poor solubility of compounds **7**−**9** led to the preparation of deprotonated versions **7a**−**9a** to extract accurate ε values. The profiles for **7a**−**9a** reveal similar profiles to the $-NO_2$ series, but the intensity of the band centered at about 410 nm (i.e., λ_{max3}) increases as the electron-withdrawing nature of the aromatic moiety increases. Consequently, **9a** exhibits the most intense and broad absorption profile in the visible region of any protonated or deprotonated complex evaluated in this study.

Although **7a** contains an additional aromatic ring relative to **1**, torsional strain between the two phenyl rings inhibits conjugation resulting in little improvement in the light-harvesting properties. The E_{ox} value is also slightly lower than that of **1a**; thus, **8a** was prepared as a means of increasing the oxidation potential. While this approach proved successful, the oxidation potential is still significantly lower than that of **6** (and **6a**), and the absorption profile was not markedly better than that of **1a** because of the adjacent six-membered rings. The installation of a thiophene group, however, proved to be a viable strategy for enhancing conjugation on the basis that the spectral profile of **9a** is more intense than that of **1a**. The presence of the aldehyde at the 2-position of the thiophene also imposes electron-withdrawing character on the substituent, which is reflected by the higher E_{ox} value relative to **8a**.

The $-NO_2$ compounds **2**−**5** are likely not ideal for sensitizing semiconducting materials because the excited-states are, in large part, quenched by the strongly electron-withdrawing substituents. The aromatic substituents of **7a** and **8a** did not produce superior photophysical properties despite the extension of the π system owing to the steric encumbrance of the adjacent six-membered rings. Compound **9a** appears to be a particularly promising candidate for the DSSC (where the anode is TiO_2 and the electrolyte is I^-/I_3^-): the E_{ox} value is higher than that of **1a**; the spectral profile is significantly more intense than that of **1a** and **6a**; and the orbital structure is poised for electron-injection and dye regeneration. Results from this study demonstrate that expansion of the HOMO is a valid strategy for producing compounds that may exceed the performance of benchmark complexes **1** and **6** reported by Grätzel et al.[30] Studies are currently underway to build on these developments and to examine their feasibility in solar cell devices.

Conclusions

The electrochemical and photophysical properties of a series of cyclometalated Ru(II) complexes related to **1** were examined to elucidate the effect of modifying the anionic fragment of the *C*^*N* ligand with conjugated substituents. It is shown that the installation of substituents *para* to the organometallic bond imparts the greatest influence on the redox behavior and optical properties. The electron-withdrawing character of the substituents are reflected by substantial changes in E_{ox} values, a consequence of extending the HOMO beyond the phenyl ring of the *C*^*N* ligand. Expansion of the HOMO over the substituent is most effective in the case where torsional strain is reduced (i.e., **9a**). In effect, this strategy produces a larger spectral envelope for **9a** relative to **1a**. The presence of an EWG on the thiophene also maintains a higher oxidation potential relative to **1a**. These collective observations provide guiding principles that are critical to the evolution of cyclometatated Ru(II) chromophores.

Acknowledgment. This work was financially supported by the Canadian Natural Science and Engineering Research Council (NSERC), Canada Research Chairs, Canada Foundation for Innovation, Alberta Ingenuity, Canada School for Sustainable Energy, and The Institute for Sustainable Energy, Environment & Economy. P.G.B. acknowledges Alberta Ingenuity for financial support.

Supporting Information Available: Labeling scheme for ligand ^{1}H NMR assignments, ^{1}H NMR spectra of **1a**, **6a**, **7a**, **9a**, UV−vis of the fully protonated aromatic series, calculated UV−vis spectra, and a summary of the TD-DFT for all compounds. This material is available free of charge via the Internet at http://pubs.acs.org.